
# Deep Learning Approach to Identify Diseases and Biomarkers in Optical Coherence Tomography Scans

**Yeison David Sanchez Legarda**

Universidad Nacional de Colombia
Systems and Industrial Engineering Department
Bogotá, Colombia
2021

# Deep Learning Approach to Identify Diseases and Biomarkers in Optical Coherence Tomography Scans

**Yeison David Sanchez Legarda**

Thesis or degree work presented as a partial requirement to apply for the title of:
**Magister en Ingeniería de Sistemas y Computación**

Advisor:
Ph.D. Fabio Augusto González
Co-Advisor:
Ph.D. Oscar Julián Perdomo Charry

Research Line:
Systems and Industrial Engineering Department
Research Group:
Machine learning, perception and discovery Lab - MindLab

Universidad Nacional de Colombia
Systems and Industrial Engineering Department
Bogotá, Colombia
2021

*To my dad David Sanchez Reyes memory, who brought me right till this point*

# Acknowledgment

I want to thank Professor Fabio González and Professor Oscar Perdomo for all their accompaniment and guidance during this process. Likewise would like to thank all the members of MindLab research group of the Universidad Nacional de Colombia who helped me and contributed with their ideas.
Finally, I would like to thank my family for all the support and patience that I was given.

# Resumen


### Enfoque de aprendizaje profundo para identificar enfermedades y biomarcadores en imagenes de tomografía de coherencia óptica

Las causas más comunes de ceguera en todo el mundo son las enfermedades de la retina, para identificarlas y no permitir que lleven a la pérdida de la visión de una persona es necesario un diagnóstico temprano, hoy en día el uso de las imágenes OCT para realizar este diagnóstico se ha incrementado debido a la capacidad de mostrar en detalle biomarcadores como fluidos, drusas, quistes y focos hiperreflectivos, sin embargo el análisis de las imágenes OCT no es fácil y consume mucho tiempo incluso para los oftalmólogos expertos lo que combinado con la sobrecarga de trabajo en el sistema de salud hace aún más difícil el diagnóstico y seguimiento de las enfermedades retinales, Con el trabajo de tesis "Deep Learning Approach to Identify Diseases and Biomarkers in Optical Coherence Tomography Scans", se propone un método para la segmentación de imágenes OCT con el fin de obtener biomarcadores que puedan ayudar al oftalmólogo a comprobar la respuesta al tratamiento o identificar una enfermedad de la retina, además se implementó un método de aprendizaje profundo para comprobar qué enfermedad está presente en una imagen.


**Palabras clave: Aprendizaje profundo, tomografía de coherencia óptica, visión por computador, aprendizaje de máquinas,segmentación de biomarcadores,clasificación de enfermedades retinianas, redes Neuronales Generativas Adversarias**.

# Abstract


### Deep Learning Approach to Identify Diseases and Biomarkers in Optical Coherence Tomography Scans

The most common causes of blindness around the world are retinal diseases, to identify them and not allow to lead to loss of vision for a person an early diagnosis is necessary, nowadays the use of OCT scans to perform this diagnostic has increased due to the capacity to show in detail biomarkers as fluids, drusen, cyst and hyperreflective foci. However the OCT scans analysis is not easy and time consuming even for experts ophthalmologist and in combination with the overload work overload in the healthcare system makes even more difficult to diagnose and follow-up the retinal disease, at this point comes in to help deep learning allowing the automated detection of diseases and biomarkers, With the thesis work "Deep Learning Approach to Identify Diseases and Biomarkers in Optical Coherence Tomography Scans," a

method was proposed to OCT scans segmentation to obtain biomarkers which can help the ophthalmologist to check response to treatment or identify a retinal disease, furthermore a deep learning method for check which disease is present in a scan was implemented.

**Keywords: Deep Learning, Optical Coherence Tomography scans, Computer vision, Machine Learning,Biomarkers Segmentation,Retinal Diseases Classification, Generative Adversarial Networks**

# Content

# List of figures

# List of tables

# 1 Introduction

Visual impairment is a congenital or acquired condition that affects a large part of the population; approximately 39.6 million people are severely visually impaired. Moreover, 279 and 969 million people are mildly or moderately visually impaired, respectively [1][2]. The leading causes of visual impairments are macular diseases which include age-related macular degeneration (AMD), diabetic macular edema (DME), and retinal vein occlusion (RVO); those diseases have received widespread attention in recent years.

AMD generally affects older people after 60 years, is a macular disease characterized by drusen and laminal deposits between retinal pigment epithelium (RPE) and Bruch's membrane (BM), causing deformation on those layers, and it can result in an irreversible loss of central vision, there are two categories for this disease which are wet and dry these can be differentiated mainly for neovascularization presence or absence [3].

DME is one of the most common retinal disorders causing vision impairment and blindness. DME is associated with diabetes because increased blood sugar levels cause damage to blood vessels producing leakage and accumulation of fluid and blood into the retina. DME can be graded into different stages according to the quantity of fluid leaked in the retina and can be prevented in early stages[4][5].

One of the precedents technologies from Artificial Intelligence (AI) that has contributed significantly to the state-of-the-art in image recognition in the medical area is Deep Learning (DL) [6], achieving outstanding results in solving several health problems. DL because of presented results helping with retinal diseases becomes essential because retinal diseases represent a significant cause of blindness worldwide in the elderly population and to people of productive ages in developing countries[7].

Within the imaging techniques used to diagnose macular diseases, the most common is eye fundus images; however, the optical coherence tomography (OCT) is most accurate and considered as the gold standard for macular disease detection [6].

The OCT scans have become widely used by experts in clinical studies in recent years due to their high resolution, providing an alternative to review cross-sectional imaging on internal layers and with this, the retinal structures and morphology enabling the detection and assessment of abnormalities on the retina including different types of findings in the retinal region such as fluids, HRFs, drusen and cysts[8][9].

The location and shape of those retinal findings provide additional information to the ophthalmologist, and it can help to grain specific macular diseases such as diabetic macular edema (DME), age-related macular degeneration (AMD), and retinal vein occlusion

(RVO)[10].
The experts assess the OCT scans considering the size, number, and location of these abnormalities, so-called biomarkers. To identify diseases can be set [11], the biomarkers include hyperreflective foci (HRF), fluids, cysts, and drusen.
HRF are signs of lipid extravasation, proteinaceous material, and inflammatory cells [12], in OCT images, those can be seen as dot-shaped lessons with a bigger or equal reflectivity than retinal pigment epithelium (RPE) and are scattered all over the retina, particularly over external layers [13] [14].
Fluids refer to the leakage of damaged blood vessels in the macular region; according to the place where the fluid is accumulated, it receives a name being intra-retinal fluid (IRF), sub-retinal fluid (SRF), and sub-retinal pigment epithelium (PED) spaces [15] [16] [17].
Fluid accumulation because of blood-retinal barrier disruption constitute areas where cells are displaced; this is also known as cysts. At last, we got drusen which are deposits of extracellular debris under the RPE layer [18].
Ophthalmologists to perform diagnose and follow-up patient progression taking decisions about the treatment of retinal diseases can be assisted with biomarkers segmentation as cysts, fluids, drusen, and HRFs in conjunction with high-resolution 3D volumes of the retina information provided by OCT scans. An early diagnosis and treatment of retinal diseases can avoid vision loss due to retinal diseases such as AMD, RVO, and DME.[15]
Early stages of retinal diseases require a treatment that includes taking nutrition supplements, controlling body weight, or avoiding cigarette smoking; for advanced stages of retinal diseases, anti-vascular endothelial growth factors (anti-VEGF) therapy is necessary; this therapy, in addition, requires regular monitoring.[19]
For the diagnose and tracking of retinal diseases is required a manual biomarker identification by ophthalmologists. However, this process is time-consuming, tedious, and error-prone even when is made by experts ophthalmologists, thus producing a heavy workload on the healthcare system due to monthly visits of patients and also a financial burden for both healthcare systems and patients[12] [9].
To achieve early identification of a disease can avoid vision loss or, in some cases blindness, also most expensive treatments. Aided automated computer methods can achieve early identification in two ways: first through classification, and secondly through the findings segmentation to help the ophthalmologist to identify the disease in early stages[20] [21].

## 1.1 Problem Identification

The severity of blindness from far it can be classified by determining the patient's visual acuity can be subordinated in mild (visual acuity less than 6/12), moderate (visual acuity less than 6/18), severe (visual acuity less than 6/60), and blindness (visual acuity less than 3/60). Regarding relative vision deficiency, it is estimated that approximately 826 million people are affected[22].

Among the risk factors that significantly influence the presence of some type of visual impairment, according to the world health organization (WHO), are the growth and aging of the population [19].
Retinal vein occlusion (RVO) and branch retinal vein occlusion (BRVO) are the most important vascular disorders and consultation prevalent after diabetic retinopathy (DR) present in the population between the sixth and seventh life decade. Literature review shows that presenting metabolic diseases such as diabetes mellitus increases the risk of visual impairment because patients can present two types of conditions which are diabetic retinopathy and diabetic macular edema. Diabetic macular edema represents the leading cause of visual loss in the condition[1].
Nowadays, clinical examination and subjective analysis of images by trained ophthalmologists are the main methods for macular diseases diagnosis such as diabetic macular edema (DME), age-related macular edema (AMD), and RVO. The two most commonly used types of diagnostic imaging are eye fundus and OCT images[23]. // OCT has shown to have a better focus over eye fundus images, ultrasound, and fluorescein angiography because OCT scans show a better resolution and suitability for clinical work support showing in detail the retinal morphology. Given the characteristics mentioned above, OCT turns out to be helpful to the health professional to choose more effectively the type of interventional treatment that the patient needs and evaluate the treatment response. Available treatment includes antivascular endothelial growth factor (anti-VEGF) and vitrectomy surgery [24].
Then we got that there are so many factors that intercede in the individual experience of patients concerning vision loss within these those that generate the most significant impact according to WHO are the availability of prevention, treatment interventions, and access to vision rehabilitation[25].
The speedup of the diagnostic process allows the early diagnosis, timely treatment of macular diseases, and facilitating decision-making by healthcare experts, increasing the number of people diagnosed and decreasing healthcare costs. Automated computed assisted methods can support the detection and diagnosis of macular-related findings and macular diseases to relieve the workload of ophthalmologists.[26]
However, the training of DL methods to automatically detects macular diseases requires large datasets. To our knowledge, there are no works that face the problem of classifying simultaneously three macular diseases such as AMD, RVO, and DME; most of the works are focused on DME and AMD detection, RVO has been an issue non-explored. The main works use support vector machines (SVM). The second great challenge that arises is the segmentation of fluids without taking into account retinal layers. By identifying the retinal layers, the area of interest for each image can be extracted and, through this segment, easily biomarkers[27][28]. To face the identified problem, the following research questions appear:

- Which are the advantages that provide us the use of deep learning for OCT images for identifying retinal diseases?

- How to measure which deep learning method has the best performance facing OCT image analysis?
- How can the quality of the fundus image be improved automatically using deep learning models?
- Which method based on deep learning allows optimal segmentation of fluids in OCT images?

## 1.2 Main and Specific Goals

### 1.2.1 Main Goals

To use deep learning to retinal diseases identification through experimentation with OCT images from different public databases.

### 1.2.2 Specific Goals

- To propose/adapt a deep learning method to biomarkers segmentation in OCT images through experimentation with annotated masks from public databases.
- To propose/adapt a deep learning method to retinal diseases classification (RVO, DME, AMD) through experimentation with annotated biomarker images.
- To systematically validate and evaluate obtained results determining the usefulness of the classification through the comparison against identified algorithms in the literature review.

## 1.3 Contributions

Several products were produced through the realization of this work, these include datasets and conference papers.

### 1.3.1 Conference papers

During the conduct of this research the following conference papers were developed :

- Segmentation of retinal fluids and hyperreflective foci using deep learning approach in optical coherence tomography scans

### 1.3.2 Datasets

- A dataset based on Duke dataset annotated with binary masks of retinal fluids [1].
- A dataset based on Duke dataset annotated with binary masks of HFs [2].

## 1.4 Thesis Structure

The remainder of this thesis is structured as follows: The second chapter presents the background and related works. The third chapter presents the first problem tackled: the biomarkers such as HRFs and fluids (intraretinal and subretinal fluids). Fourth chapter shows second tackled problem which is based on drusen,cyst HRFs AND fluids also the also OCT image classification for diseases like DME, AMD and RVO. Finally, the fifth chapter presents the thesis conclusions and ideas for future work.

[1] https://github.com/yeisonlegarda/fluidsdukemarkeddataset
[2] https://github.com/yeisonlegarda/focisdukemarkeddataset.git

# 2 Related Works

## 2.1 OCT images classification

The leading causes of visual impairments are macular diseases, among which can be found age-related macular degeneration (AMD), diabetic macular edema (DME), and retinal vein occlusion (RVO); those diseases have received widespread attention in recent years. AMD generally affects older adults after 60 years, existing two categories for this disease which are wet and dry those are mainly differentiated for neovascularization presence or absence [3][29], DME it's one of the most common retinal disorders associated with diabetes because of increased blood sugar levels damage blood vessels producing leakage and accumulation of fluid and blood into the retina [4] [5], table **2-1** shows the summary of work done for the topic of disease classification with OCT scans.

### 2.1.1 AMD classification

Khalid et al. [30] proposed a fusion method that consists of image denoising and layer extraction from OCT images. First, the RPE layer is extracted from the image. Some characteristics such as minimum, maximum, variation, energy surface, and zero crossings are stratified from this layer. Zero-crossings characteristics provide information about drusen. An SVM classifier is trained using these features to classify an image into healthy or ARMD (Age-related macular degeneration) suspect. If the OCT image is classified as a suspect, then the fundus image is used to confirm an early warning or if the subject already has the disease. After this process, drusen areas in fundus images are extracted using Otsu thresholding algorithm. If the drusen appear on both images, the subject is classified as suffering from ARMD. Maximilian et al. [31] proposed a model based on Inception-v3 architecture, where the last layer allows to detect exudative AMD or healthy images.
Naohiro et al. [24] crop OCT scans into three patches and uses two CNN to classify the image between AMD, normal, with, or without exudative change. At last, the three patches are joined to obtain the original image classification, class activation mapping (CAM) was applied on both CNN to get the pathological region on the image. On the other hand, Serener et al. [32] analyzed two different architectures: Alexnet and ResNet to predict between dry and wet AMD looking best results with ResNet.
Sun et al. [23] performed fine tunning on RESNET50 to feature extraction over OCT volumes labeled as AMD, DME, or healthy. The feature extraction gives a 2-D vector for a slice that

is stacked with others of volume. All volumes are classified by three models those are CNN, CNN with convolutional block attention module (CNN_CBAM) and SVM. The use of SVM and CNN_CBAM provided better results than other proved methods. Alqudah et al. [33] take a different approach which consists of preprocessing images and using double-density wavelet transform-based adaptive thresholding and propose and CNN architecture to classify OCT images among AMD, CNV, DME, drusen, and normal labels.

In 2021, Zhiyan et al. [3] reported a model that combines two eye imaging (OCT and fundus) to improve previous results. This method used a DCNN with two inputs, an OCT image and a fundus image. For training, imageNet weights on RESNET-50 are loaded and fine-tuned on a separated model. The fine tunned models are unified in a single network for feature extraction and to classify between wet AMD, dry AMD, Polypoidal choroidal vasculopathy (PCV).

### 2.1.2 DME classification

For DME classification task, some works have been done. In 2019 Hassan et al.[2] fuses OCT and fundus images, where two CNNs perform feature extraction for each individual source of information. These features are concatenated, and an SVM is trained to perform the classification. Moura et al.[1] took a similar approach when using CNNs as AlexNet, VGG-19, and Inception-V3 to feature extraction and an SVM to perform classification, where the best results were achieved by using VGG-19.

Ibrahim et al.[4] applied sparsity-based block-matching and 3D-filtering (BM3D) to denoise images. Then a modified VGG16 is used to generate heat maps and performs ROI extraction around the generated mask with red and yellow colors on the map. Features were extracted by Histogram of Oriented Gradients (HOG), and DAISY feature descriptor is combined with VGG16 and provided to a Neural Network (NN) to classify between CNV, DME, drusen, and normal. Aya et al [5] performed transfer learning on Inception V3 and Xception architectures training last ten layers to classify between normal, Choroidal neovascularization CNV, DME.

### 2.1.3 RVO classification

As far as we know, there are not many works on RVO classification most recent was conducted by Daisuke et al., [34] who making use of two approaches, SVM and a DNN architecture known as VGG-16, to classify images between RVO and non-RVO. Data augmentation is performed over images performing brightness adjustment, noise changes, and gamma correction. For classification, the best performing method was the DNN. At last, for determining nonperfusion area (NPA), a heatmap was employed using a gradient-weighted class activation mapping (Grad-CAM) over VGG-16.

## 2.2 OCT scans segmentation

The classification of AMD, DME, and RVO diseases and the location of clinical findings related to these diseases is a clinical challenge because the agreement among experts is based on the years of expertise in retina [8][9]. Some experts perform a screening through the OCT volume looking for in each scans amount of findings and location of these abnormalities called biomarkers to identify diseases [11]. Thus, an early diagnostic and proper treatment must be performed by experts to avoid loss of vision due to retinal diseases such as AMD, RVO, and DME. So, the automatic and accurate identification of these biomarkers is vital to diagnoses and follow-up patient progression. Deep learning methods have shown outstanding results in locating and segmentation biomarkers such as fluids, cyst, drusen, and HRFs. However, these works only tackle individual biomarkers in most cases, and reports with all of these biomarkers are not found. Table **2-2** presented a summary with the most representative works on the segmentation task of macular biomarkers.

### 2.2.1 HRFs segmentation

Schlegl et al. [13] proposed a generative adversarial network to biomarkers segmentation in those biomarkers includes HFRs and fluid. This model was trained to extract retinal layers for the image, using a residual loss for the discriminator, which allows the generator to provide images with similar statistics as the training data. Thus the network is trained with healthy images to identify anomalous regions on the image a residual image is calculated. The proposed method name is AnoGAN.

Then, Schlegl et al. [35] proposed another approach that applied some architectures as SemSeg, ResUnet, and ResUnet plus with cross-entropy loss and dice loss. Semseg network contains encoder and decoder blocks with layers of size 16-64-64-128 and 3x3 filters. The ResUnet is a UNET architecture with residual blocks on it. Those residual units allow learning the residual functions between inputs and outputs, not only the mapping of those. At last, the ResUnet plus includes one more block on the encoder and decoder. The best-obtained results were for ResUnet Plus. Katona et al.[36] performed the detection of pigment epithelial detachment (PED), outer retinal tubulation (ORT), looking for HFRs; through the application of Weiner filter and localizing points with a hessian detector. For HFRs segmentation, they arent focus on segmenting and taking the changes in the HFRs amounts, so they use standard Artificial Neural Networks (ANN), Deep Rectifier Neural Networks (DRNN), and convolutional neural networks. For ANN and DRNN, training is given to network two input types: the raw pixel data with intensities of the vicinity. The second input is about features like a weighted sum of pixel intensities in the neighborhood.

Varga et al. [14] tested eight different models for HRFs segmentation; images from OCT-scans are converted into black-on-white, for DRNs and ANN feature vectors are extracted. Feature vectors have got the raw pixel information, intensity, and 23X23 vicinity, the in-

formation provided by filters as Laplacian of Gaussian (LoG), the distance between the processed pixel and internal limiting membrane (ILM), Retinal Pigment Epithelium (RPE), and intraretinal fluid accumulation (IRF), the calculation about the difference between HF and blood vessels and pigment particles. With this information, networks are trained, for CNNs and Fully Convolutional Neural Networks (FCN), image patches of 23 X 23 are passed. Yu et al.[37] Uses a Deep Convolutional network, applying on the image a bilateral filter and taking patches of 33 X 33, 65 X 65, 85 X 85, and 115 X 115, manually deleting false focis. The networks used are GoogleNet and Resnet. The best model was GoogleNet, with patches of 65x65.
In 2020, Xie et al.[12] using a bilateral filter and sigmoid transfer function follow by histogram equalization to enhance images. Network architecture is trained with image patches of 128X128X3, to 3D UNET are integrated dilated convolutions to capture multiscale and low range information. Moraes et al. [38] used a similar approach using OCT scans and demographics information about patients. This data is passed through a 3-dimensional segmentation network. The segmentation network uses 2d convolutions; analyzing features as the neurosensory retina (NSR), retinal pigment epithelium (RPE), IRF, SRF, subretinal hyperreflective material SHRM, hyperreflective foci (HRF), drusen, fibrovascular pigment epithelium detachment (fvPED), and serous PED (sPED). For images, the biomarkers are measured after treatment, noticing that except by drusen, biomarkers decrease.
Finally, Okuwobi et al.[**?**] used a bilateral filter to denoise the OCT images. After denoising ROI extraction and HFs quantification is performed, the ROI extraction is made through fuzzy c-means clustering. For HFs estimation, an algorithm has been proposed that works through voxel ordering and adding those into a forest to remove duplicated and redundant regions. At last, these two processes are merged.

### 2.2.2 Fluids segmentation

Fluids segmentation is one of the areas with the most developed works, and it can be seen that most of those works in the first few years use graph theory to perform segmentation. Xu et al.[39] used a non-linear three-dimensional anisotropic diffusion filter and sequence of brightness curve transform to image denoising this allows to differentiate the layers of retina and biomarkers, continuing with the taking of subregions called strata and a set of features are calculated those include textural, structural, and positional information, for testing it was used a k-nearest-neighbor classifier, this method allows to classify even small regions, however, the method provided depends on retinal layer segmentation, if segmentation is poorly made, results are bad. Oguz et al.[27] reported the segmentation with Boykov graph cut algorithm with node costs given by a weighted sum of a layer-dependent Mahalanobis intensity distance and the skewness measure. In the same way, Rashno et al [16] employ graph theory placing the images in a neutrosophic domain and after this, for segmentation of first and last layer a method based on graph shortest path is applied, for fluid segmentation

is applied a method based on graph cut, to increase segmentation accuracy design a cost function based on kernel mapping.
Roy et al [40] perform multiclass segmentation for retinal layers and fluids through a deep learning framework based on a fully convolutional network named Retinal Layer segmentation network (ReLayNet) this network incorporates unpooling stages with skip connections for image segmentation. Schlegl[35] with OCT images from different vendors and diseases as AMD, DME, and RVO, propose a network with encoder and decoder path to classify pixel into three classes intraretinal fluid, subretinal fluid, and normal tissue. Tennakoon et al. [15] propose an adversarial network with a generator network based on UNET, also use a combined loss function consisting of an adversarial loss term.
Seebock et al. [21] process images for different vendors to make domains as equals as possible with an algorithm using mean filter operation with a kernel size of 3x3 and another mean filter with a kernel of size 1x1x3 and histogram matching using spectralis OCT volumes as a template, after transformations a CycleGANs with two generators and two discriminators was applied, the fist pair generator discriminator works for domain translation, the second one performs fluid segmentation, there were trained four models with patches of 64,128,125 and 460, the best result was for patches with size 460.
Wen et al. [23] proposed an improvement for UNET based on multiscale input, two architectures named 16 and 32 were proposed these numbers denote the number of convolutional kernels in the first encoder block, to train the network was used a joint loss function was based on weighted multi-class cross-entropy and dice loss. Then, Chen et al, develop a modification over UNET but this time the modification involves adding Squeeze-and-Excitation block (SE-block) on the entire network, this method uses a graph-based segmentation to extract retinal layers, subsequently as preprocessing stage the BM3D algorithm to image denoising and color reversing was used, after fluid segmentation images are classified into normal or AMD depending on whether the image has got fluid pixels.
Xiaoming et al [9] performed the automated fluid segmentation based on a modified UNET which has got an encoder a two decoder paths with attention gates, also was tried a regression loss, this model was trained using image patches of 256 x 256.

### 2.2.3 Cyst segmentation

As mentioned in the previous sections, the cyst segmentation case applied methods include graph theory, SVM, and CNN networks. Oguz et al. [27] presented a graph optimization for image segmentation method where a node in a graph represents each voxel and assigning weights according to the terminal and neighboring nodes. Once the graph is built, to find the optimal solution max-flow algorithm is used. Meanwhile, Gopinath et al. [10] employs total variational denoising. After this, ROI is extracted using maximally stable extremal regions(MSER), and on the extracted region is used a random forest with 50 trees to classify between a cyst and no cyst regions.

Girish et al.[41] to denoise image used an Unbiased Fast Non-Local Means (UFNLM), and for image segmentation is used an FCN based on UNET. Gopinath et al. [42] introduce a total variational denoising method and using an ensemble between Generalized Motion Pattern (GMP) and a CNN model, which learns a function to produce a probability map with pixels having a significant probability of benign cysts.
Girish et al. [43] applied Bayesian non-local means (BNLM) filter to denoise images. Also, retinal layers are segmented using optical coherence tomography segmentation and evaluation GUI tool; for intra-retinal cysts segmentation was used a marker-controlled watershed transform; for cyst segmentation, a k-means algorithm performs some post preprocessing stages, selecting a cluster with minimum centroid and removing segmented outlier regions.

### 2.2.4 Drusen segmentation

For drusen, some other works were carried out as Rui et al.[19] that with a directional graph search method perform Bruch's membrane segmentation, and with a hybrid contrast map, separate healthy OCT scans for those that have drusen. In the last step, Top-Hat transform and Otsu thresholding are used to extract drusen, also a median filter to generate the definitive drusen area. Some other jobs are mainly based on UNET. As for Rhona et al.[44] who uses a UNET model modifying it with pyramid feature maps and making use of dice loss function to segment the outer boundary retinal pigment epithelium (OBRPE), Bruch's membrane (BM), and drusen as an external class. Also, in 2019 Shekoufeh et al. [18] employed a U shape model to perform multiclass using the same encoder and different decoders to make binary classification and join those results.
Mishra et al. [28] used a UNET model to produce probability maps of layer, drusen, and interest regions in OCT images. With those probability maps, a graph-based method was used to calculate path shortest path with Dijkstra's algorithm in junction with SD-OCT scan gradient to determine layer segmentation, and a cubic spline fitting was used to correct small segmentation error.

**Table 2-1**: State-of-the-art summary for disease classification over OCT images

| Year | Reference | Disease | Method | Dataset |
|---|---|---|---|---|
| 2018 | [30] | AMD | Image denoising and layer extraction from OCT images, after feature extraction SVM is used to classify an image into healthy or ARMD (Age-related macular degeneration) suspect, if the image is classified as suspect then fundus image is used to confirm an early warning or if the subject already has the disease. | Private |

| | | | | |
|---|---|---|---|---|
| 2018 | [45] | AMD | Graph theory, watershed transform, and CNN to identify biomarkers and combine those with demographic information passing into a sparse Cox proportional hazards (CPH) model regularized by least absolute shrinkage and selection operator (LASSO). | Private |
| 2018 | [31] | AMD | Inception-v3 training last layer to detect exudative AMD or healthy images. | Private |
| 2019 | [24] | AMD | Crop the OCT image into three patches and uses two CNN to classify the image between AMD and normal, second CNN classifies the image into with or without exudative change, at last, the three patches are joined to obtain the original image classification, class activation mapping (CAM) was applied on both CNN to get the pathological region on image | Private |
| 2019 | [32] | AMD | Alexnet and ResNet architectures to predict between dry and wet AMD, ResNet proves to get better results | Private |
| 2019 | [2] | DME | Train an AlexNet architecture to distinguish between OCT and fundus images than by using Wiener filter images are denoised and using structure tensor interest region was extracted, with a CNN performs feature extraction, and using neural networks and SVM perform the classification, the best result is given by mixing feature extraction with CNN and classification with SVM | Private |
| 2019 | [1] | DME | AlexNet, VGG-19 and Inception-V3 to feature extraction and a SVM to perform classification, best results were achieved by using VGG-19. | Private |

| | | | | |
|---|---|---|---|---|
| 2019 | [34] | RVO | SVM and a DNN architecture known as VGG-16 to classify images between RVO and non-RVO, data augmentation its performed over images performing brightness adjustment, noise changes, and gamma correction, for classification the best performing method was the DNN, at last, for determining nonperfusion area (NPA) was employed a heatmap using a gradient-weighted class activation mapping (Grad-CAM) over VGG-16. | Private |
| 2020 | [23] | AMD | Fine tunning on RESNET50 to feature extraction over OCT volumes labeled as AMD, DME, or healthy, the feature extraction gives a 2-D vector for a slice which is stacked with others of volume, all volumes are classified by three models those are CNN, CNN with convolutional block attention module and support vector machine (SVM), the use of SVM and CNN_CBAM provides better results. | Private, Duke[46] |
| 2020 | [33] | AMD | Image denoising with double-density wavelet transform-based adaptive thresholding and propose and CNN architecture to classify OCT images among AMD, CNV, DME, drusen, and normal labels. | Private, Duke[46] |
| 2020 | [4] | DME, CNV | Sparsity-based block-matching and 3D-filtering (BM3D) to denoise images, then a modified VGG16 is used to generate heat maps and performs ROI extraction around the mask generated by red and yellow colors in a map, with this extracted ROI features extracted by Histogram of Oriented Gradients (HOG) and DAISY feature descriptor are combined with VGG16 and provided to a Neural Network (NN) to classify between CNV, DME, drusen and normal | Private |

| | | | | |
|---|---|---|---|---|
| 2020 | [5] | DME,CNV | Transfer learning on Inception V3 and Xception architectures training last ten layer to classify between normal, Choroidal neovascularization (CNV), DME | Private |
| 2021 | [3] | AMD, PCV | DCNN with two inputs an OCT image and a fundus image, for training weights from imageNet on RESNET-50 are loaded and fine-tuned on a separated model, the fine tunned models will be unified in a single network for feature extraction and to classify between wet AMD, dry AMD, Polypoidal choroidal vasculopathy (PCV) and normal | Private |

**Table 2-2**: State-of-the-art summary for biomarkers segmentation (Fluids,HRFs,Cyst,Drusen) on OCT images

| Year | Reference | Biomarker | Method | Dataset |
|---|---|---|---|---|
| 2015 | [39] | Fluid | Non-linear three-dimensional anisotropic diffusion filter and sequence of brightness curve transform to image denoising this allow to well seeing the layers of retina and biomarkers, the method is based on taken subregions called strata and a set of features are calculated those include textural, structural, and positional information, and for testing it was used a k-nearest-neighbor classifier | Private |
| 2016 | [27] | Cyst | Median filter for image denoising and retinal layer segmentation, after those steps each voxel in the image represents a graph node, and the weights between the node and terminal and neighborhood nodes represent regulation constraints and image appearance, with this graph construction a max-flow algorithm it's used to perform segmentation. | OPTIMA[47], Duke[46] |

| | | | | |
|---|---|---|---|---|
| 2016 | [10] | Cyst | total variational denoising to image denoising, after this its extracted ROI using Maximally stable extremal regions(MSER) and on the extracted region it's used a random forest with 50 trees to classify between a cyst and no cyst regions. | OPTIMA[47] |
| 2017 | [11] | Drusen | U-NET model to extract the Bruch's membrane (BM) and the retinal pigment epithelium (RPE) layer and after segmenting it its used Dijkstra's algorithm to connect boundaries with minimum cost also takes another approach this time segmenting the space between layers and based on layer on both cases drusen are detected by rectification, polynomial fitting, and thresholding. | Private |
| 2017 | [19] | Drusen | Directional graph search method Bruch's membrane was segmented with a hybrid contrast map healthy OCT scans are separated for those that have drusen in the last step is used Top-Hat transform and Otsu thresholding to extract drusen the segmentation has got some corrections which include a logical or and also a median filter to generate the definitive drusen area | Private |
| 2017 | [13] | HRFs | Generative adversarial network to biomarkers segmentation in those biomarkers includes HFRs and fluid, the networks were trained extracting retinal layers for image, for training the networks it's used a residual loss for the discriminator and a loos on discriminator which allows the generator to provide images with similar statistics as the training data and generating an anomaly score which indicates that a similar image was seen during the training phase, thus the network is trained just with healthy images, to identify anomalous regions on the image a residual image its calculated, the proposed method its called AnoGAN | Private |

| | | | | |
|---|---|---|---|---|
| 2017 | [40] | Fluid | Multiclass segmentation for retinal layers and fluids through a deep learning framework based fully convolutional end-to-end called Retinal Layer segmentation network (ReLayNet) this network incorporates unpooling stages with skip connections for image segmentation the oct scan is sliced widthwise. | Duke[46] |
| 2017 | [16] | Fluid | Graph theory-based image segmentation, but the images in a neutrosophic domain and after this, for segmentation of first and last layer a method based on graph shortest path is applied, then for fluid segmentation it's applied a method based on graph cut and for increase segmentation accuracy designs a cost function based on kernel mapping. | OPTIMA[47], UMN[16] |
| 2018 | [15] | Fluid | Adversarial network with a generator network based on UNET also as loss function use combined loss function consisting of a adversarial loss term, | RETOUCH [48] |
| 2018 | [35] | Fluid | OCT images from different vendors and diseases as AMD, DME, and RVO, propose a network with an encoder-decoder path to classify pixel into three classes intraretinal fluid, subretinal fluid, and normal tissue | Private |
| 2018 | [49] | Fluid | GAN network to perform retinal layers and fluid segmentation, the generator segmentation network is designed as a UNET but inspired in RelayNet which allows multiclass segmentation, the discriminator network is a fully convolutional architecture that is modified for segmentation thus the output of discriminator it's a matrix with the same size of the input image when training network for discriminator a spatial cross-entropy loss is used. | Duke[46] |

| | | | | |
|---|---|---|---|---|
| 2018 | [35] | HRFs | Architectures as SemSeg, ResUnet, and ResUnet plus with cross-entropy loss and dice loss, Semseg network contains encoder and decoder blocks with layers of size 16-64-64-128 and 3x3 filters; the ResUnet is a UNET architecture ith residual blocks on it, those residual units allows to learn the residual functions between inputs and outputs not only the mapping of those, and at least the ResUnet plus which includes one more block on encoder and decoder. | Private |
| 2018 | [36] | HRFs | Detection of pigment epithelial detachment (PED), outer retinal tubulation (ORT) looking for HFRs through the application of Weiner filter and localizing points with a hessian detector; for HFRs segmentation they arent focus on segmenting but also on tacking the changes in the HFRs amounts, so they use standard Artificial Neural Networks (ANN), Deep Rectifier Neural Networks (DRNN) and convolutional neural networks, for ANN and DRNN training it's given to network two input types: the raw pixel data with intensities of the vicinity, the second input it's about features like a weighted sum of pixel intensities in the neighborhood, the distances from layers and fluid and intensities from 40 pixel long vertical strips. The best obtaining results are from CNN | Private |

| | | | | |
|---|---|---|---|---|
| 2018 | [45] | HRFs, Drusen | Segmentation over Drusen and HRFs, drusen were segmented using a threshold over drusen thickness to detect those, also was applied a watershed transform to get individual drusen, for HFRs it was used a convolutional neural network, information about drusen, HFRs and demographic and genetic features as age, gender, smoking status and some risk alleles of single-nucleotide polymorphisms, a predictive model using sparse Cox proportional hazards (CPH) is set | Private |
| 2019 | [21] | Fluid | For two different vendors with AMD, DME, and RVO images to make domains as equals as possible uses mean filter operation with a kernel size of 3x3 and another mean filter with a kernel of size 1x1x3, after that an initial histogram matching using spectral OCT volumes as a template, after transformations a CycleGAN with two generators and two discriminators its applied, the fist pair generator discriminator works for domain translation, the second one performs fluid segmentation, there are trained four models with patches of 64,128,125 and 460 best result are for patches with size 460 | Private |
| 2019 | [50] | Fluid | Three phases are used to simultaneous segment three-class retinal fluid (IRF, SRF, and PED), first with graph cut the retinal layers are extracted, second with a multiclass FCN IRF, SRF, and PED are segmented, this FCN it's like a UNET network but receives two channels one containing a relative distance map with image intensity information, and also some changes in the last path to avoid overfitting and lastly, three random forest classifier it's used to avoid oversegment, one random forest per each type of fluid | RETOUCH [48], Kermany[51] |

| | | | | |
|---|---|---|---|---|
| 2019 | [52] | Fluid | 3D UNET to have into account correlation of the spatial position between the OCT images, in this network input and output are changed from a 2D image to a 3D image, also all convolutional kernels are 3D structures | Private |
| 2019 | [18] | Drusen | U-NET model to segment to segment retinal pigment epithelium (RPE) and Bruch's membrane (BM) and this is turned into a cost map on those its used Dijkstra's algorithm to connect images for RPE and BM with minimum accumulated cost in the cost map. lastly are performed to steps to get drusen segmentation are: rectification and final false positive elimination. | Private, Duke[46] |
| 2019 | [44] | Drusen | U shape model for performing multiclass using the same encoder and different decoders to make binary classification and join those results | Private |
| 2019 | [41] | Cyst | Unbiased Fast Non-Local Means (UFNLM) to image denoising, inspired by Google's Xception network taking depthwise separable convolution layers to propose a DSCN architecture | OPTIMA[47] |
| 2019 | [42] | Cyst | Total variational denoising method and using an ensemble between Generalized Motion Pattern (GMP) and a CNN model which learns a function to produce a probability map with pixels having a major probability of benign cysts. | OPTIMA[47], Duke[46], Private |

| | | | | |
|---|---|---|---|---|
| 2019 | [14] | HRFs | Try 8 models for HRFs segmentation, images from OCT-scans are converted into black-on-white, for DRNs and ANN feature vectors are extracted, those have got the raw pixel information, intensity, and 23X23 vicinity, the information provided by filters as Laplacian of Gaussian (LoG), the distance between the processed pixel and internal limiting membrane (ILM), Retinal Pigment Epithelium (RPE) and intraretinal fluid accumulation (IRF), the calculation about the difference between HF and blood vessels and pigment particles, with this information networks are trained, for CNNs and Fully Convolutional Neural Networks (FCN) image patches of 23 X 23 are passed, the best result were given by FCN. | Private |
| 2019 | [37] | HRFs | Deep Convolutional network, applying on the image a bilateral filter and taking patches of 33 X 33, 65 X 65, 85 X 85, and 115 X 115 manually deleting false foci, networks used are GoogleNet and Resnet, best model uses the GoogleNet with patches of 65x65 | Private |
| 2020 | [43] | Cyst | Bayesian nonlocal means (BNLM) filter to denoise the image, also retinal layers are segmented using optical coherence tomography segmentation and evaluation GUI tool, Marker controlled watershed transform for intra-retinal cysts segmentation from optical coherence tomography B-scans, for cyst segmentation a k-means algorithm performing some post preprocessing stages as selecting cluster with minimum centroid and removing segmented outlier regions was used | OPTIMA[47] |
| 2020 | [53] | Fluid | Fully convolutional neural network (FCNN) which name depth max pooling-based network (DMP Net), and in conjunction with mutex dice loss (MDL), allows to segment retinal layers and fluids. | Duke[46] |

| | | | | |
|---|---|---|---|---|
| 2020 | [54] | Fluid | Convolutional neural network and its transfer learning for another study over fluid segmentations, after that, training the network with vertically sliced OCT images. | Private |
| 2020 | [23] | Fluid | Improvement for UNET based on multiscale input, a nested Unet shape, and multiscale output and labeling, two architectures were proposed 16 and 32 that denotes the number of convolutional kernels in the first encoder block, for training the network it used a joint loss function based on weighted multiclass cross-entropy and dice loss, best performances were for MDAN-UNet-32. | Duke[46] |
| 2020 | [20] | Fluid | Graph-based segmentation to extract retinal layers, BM3D algorithm to image denoising and color reversing as the preprocessing stage, the proposed network to perform segmentation is a UNET with Squeeze-and-Excitation block (SE-block) integrated after fluid segmentation images are classified into normal or AMD images if the predicted image has got fluid pixels in it | UMN[16] |
| 2020 | [8] | Fluid | Transforms the image into a Neutrosophic (NS) domain and with Dijkstra algorithm calculates inner limiting membrane (ILM) and retinal pigmentation epithelium (RPE) layers for model segmentation and proposes an FCN structure with encoder a decoder with a depth of 4 for each one. | UMN[16] |
| 2020 | [8] | Fluid | Puts images in an NS domain, and extracts ILM and RPE layers as ROI and the middle layers outer plexiform layer (OPL) and inner segment myeloid (ISM) are segmented using the proposed graph shortest path, for fluid segmentation a clustering method it is used accompanied by a cost function derived from fuzzy c-means clustering | UMN[16], Duke[46], OPTIMA[47] |

| | | | | |
|---|---|---|---|---|
| 2020 | [55] | Fluid | Denoising images with BM3D algorithm with a sigma value of 25, and with use of FCNNs such as VGG16, Alexnet, and GoogLenet and also DCNNs as UNET, SegNet and Deeplabv3+ performs images segmentation, for DCNNs a post-processing stage was applied which consists of a median filter | OPTIMA[47], RETOUCH [48] |
| 2020 | [56] | Fluid | UNET modified network which got five contracting and expanding paths with 3X3X3 convolutions, for training using weighted cross-entropy as the loss function. | RETOUCH [48] |
| 2020 | [28] | Drusen | UNET model to produce probability maps of layer, drusen, and interest regions in OCT images, with those probabilities, maps a graph-based method is used to calculate path shortest path with Dijkstra's algorithm in junction with SD-OCT scan gradient determine layer segmentation and a cubic spline fitting is used to correct small segmentation error. | Private |
| 2020 | [12] | HRFs | Bilateral filter and sigmoid transfer function follow by histogram equalization to enhance images, then network architecture is trained with image patches of 128X128X3, to 3D UNET are integrated dilated convolutions to capture multiscale and low range information, in the last layer of encoder path | Private |
| 2020 | [**?**] | HRFs | Bilateral filter to denoise the image, after denoising ROI extraction and HFs quantification its performed, the ROI extraction made through fuzzy c-means clustering, for HFs estimation is proposed an algorithm that works through voxel ordering and adding those into a forest to remove duplicated and redundant regions, at last, this two processes are merged, | Private |

| | | | | |
|---|---|---|---|---|
| 2021 | [9] | Fluid | Modified UNET which has got a encoder a two decoder paths with attention gates, also its tried a regression loss,this model was trained using image patches of 256 x 256 | OPTIMA[47] |

# 3 Segmentation of retinal fluids and hyperreflective foci using deep learning approach in optical coherence tomography scans

This chapter explores the segmentation of fluids and HRFs through the experimentation with a publicly available dataset known as UMN that provided us with mask annotated images for intraretinal fluids and subretinal fluids, we also explored the segmentation task in the Duke dataset which only provided us with OCT scans. The OCT scans from Duke dataset were annotated by an expert ophthalmologist from the ophthalmology department of Universidad Nacional de Colombia.

In segmentation tasks of fluids and HRFs, should be considered previous works such as the one carried out by Abhijit Guha Roy et al. [40] who proposed an architecture composed of two blocks encoder-decoder and classification block to classify named RelayNet, where each pixel between ten classes belonging to layers and fluids. Sung Ho Kang et al. [57] fused two UNets, the first one makes normal segmentation, and the second one takes the segmented image and output to provide a result segmentation. Gao et al. [58] designed a double branched fully convolutional network to automatically segment fluid and hyperreflective foci in OCT images. In addition, Liling Guan et al [59] created a backbone based on ResNet-50 to delimit contours using the Distance regularized LSE (DRLSE) modified curvature diffusion equation (MCDE). László Varga et al [14] tested four layers with a RELU activation termed FCN to perform HFs segmentation. Chenchen Yu et al [37], made some changes over GoogLeNet and ResNet to segment images processing patches of those. Zailiang Chenab et al [20] suggested the use of squeeze and excitation blocks over an UNet, after applying a denoising algorithm known as BM3D all processes to improve the results provided by the UNet model. At last, Idowu Paul Okuwobi et all [**?**] implemented the use of a component tree to classify pixels previously filtering the images by an algorithm that uses morphological reconstruction to preserve edges and main images characteristics. This work was published in the *16th International Symposium on Medical Information Processing and Analysis, 2020.*

## 3.1 Introduction

Retinal diseases are the main risk factors that significantly influence the presence of some type of visual disability in childhood. The detection of those diseases in early stages may help to prevent vision loss or blindness [60]. Currently, the diagnosis of retinal diseases such as diabetic macular edema (DME), age-related macular degeneration (AMD), central retinal vein occlusion (CRVO), and branch retinal vein occlusion (BRVO) is mainly based on clinical examination and analysis of ocular images by trained ophthalmologists [61].

OCT is the most reliable image used by experts to assess the whole morphology of the retina [62]. The ocular examination is summarized as follows: the ophthalmologists look for some findings in images such as hyperreflective foci, fluids, cysts, and drusen. Then, according to the finding's position and size in the OCT, they perform the diagnosis of retinal disease [63]. The proper detection helps experts to apply effectively the interventional treatment and follow-up that the patient needs, such as antivascular endothelial growth factor (anti-VEGF) and vitrectomy surgery that improves the patient's response to treatment.

Deep learning has achieved outstanding results in the last 9 years in computer vision task [35]. Due to the successful results, deep learning has been studied as an automatic diagnostic process in screening programs to allow remote identification of ocular diseases that relieves the workload of ophthalmologist [64]

## 3.2 Methodology

The overall pipeline to segment OCT scans contains two stages. The first block is the preprocessing stage that performs the Region of Interest (RoI) extraction from scans, after resizing the scan to a resolution of $256 \times 256$ keeping aspect ratio and, the application of transformation on the resized scan and its respective mask (data augmentation. The second stage integrates two CNNs into an ensemble model. The first CNN is a Pix2Pix model and the second CNN is a modified deep retinal understanding model (DRIU) [65] as shown in Figure **4-1**.

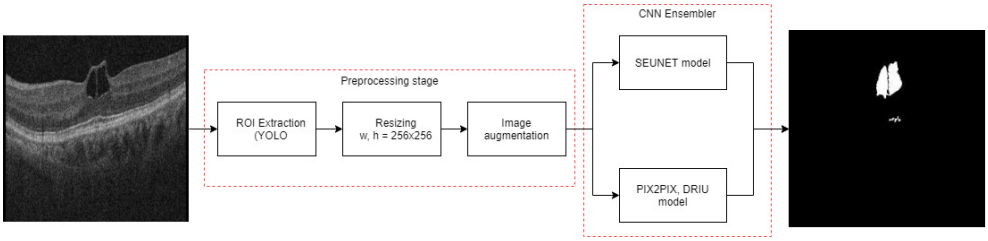


**Figure 3-1**: Block diagram of the proposed method to fluid and HFs segmentation.

### 3.2.1 Preprocessing stage

The RoI detection in all scans was performed to extract the relevant information used to feed our CNN ensembled. The RoI extraction was done with a YOLO object detection model [66]. This model was trained with 1000 images from the Duke dataset where were manually labeled with a bounding box that comprises the whole retinal layers. The output of the RoI detection model is the coordinates of the bounding box that closed retinal layers of each scan. After, the scans and the mask with the fluids and HFs were cropped according to each bounding box. The cropped scans and masks were resized into a resolution of $256 \times 256$. These resized images were used to apply transformation such as shearing, zooming, and horizontal flip on images and mask at the same time to augment the data.

### 3.2.2 Deep learning ensemble method

SEUNet is a CNN model based on UNet but with the integration of Squeeze-and-Excitation blocks (SE-block). These blocks enhanced feature maps allowing give better results than a simple UNet [20]. The DRIU architecture is a deep learning model based on VGG-19 CNN used for the segmentation of optic disc and blood vessels in eye fundus images [65]. The modified DRIU model contains squeeze and excitation blocks in the last layers to improve the performance in the segmentation task. The Pix2Pix architecture allows applying the translation of features from an image to another image. This model has been used in tasks as colorizing images and reconstructing objects from diverse representations [67]. In particular, Pix2Pix was used in retinal fluid and HFs segmentations to learn the representation of the segmented images. Pix2Pix architecture contains two stages: a generator and a discriminator, the generator stage is similar to UNet CNN but adding skip connections between blocks to help the generator avoids bottlenecks; the discriminator stage keeps the same function played in a GAN model to discriminate between real data and data created by the generator. A Patch-GAN was implemented as the discriminator in the Pix2Pix model to force low-frequency correctness.
Our proposed approach contains a SEUNet model ensembled with a modified DRIU architecture and a Pix2Pix. The motivation for the model is that the combination of these architectures may improve the detection of small lesions. In particular, SEUNet and Pix2Pix models have the best prediction in lesions with medium and large sizes. Otherwise, the modified DRIU shows the best performance in lesions with small sizes.

### 3.2.3 Dataset

The Duke dataset is a free public available dataset that contains 384 spectral domain-OCT volumes from subjects control and AMD conditions [68]. We analyzed the whole dataset to select a representative subset of 10 subjects varying from 9 to 21 images OCT scans per subject. The scans were manually labeled by an ophthalmologist obtaining 209 scans with

retinal fluids and HFs. Then, this subset was randomly split into three data sets with 70% of scans for the training set, 10% for the test, and the remaining of the sample for the validation set. The distribution of scans was the following: 146 scans for training, 42 scans for validation, and 21 for the test set, in image **4-3** from the Duke dataset are shown joined to expert ophthalmologist segmentation.

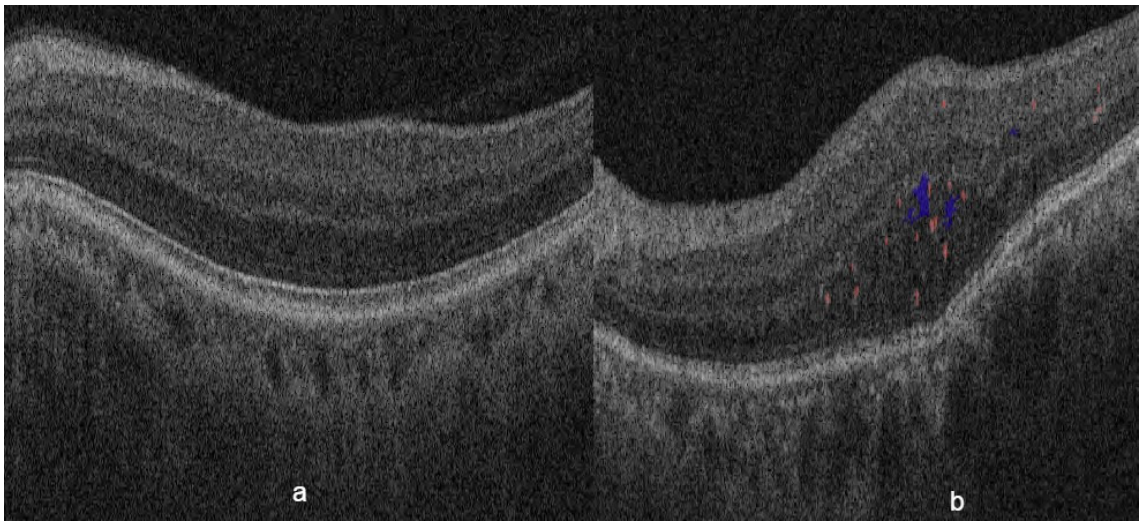


**Figure 3-2**: a) Scan without findings, b) Scan with fluids (blue) and HFs (red).

### 3.2.4 Evaluation

The performance metric used to evaluate our results was the Dice coefficient as formulated in eq. 4-1. The Dice coefficient is a statistical measure to analyze the similarity between two images. The Dice measure a range between 0 and 1, where closer values to 1 represent the most similarity between the predicted image and real segmented image [55].

$$DSC = \frac{2TP}{2TP + FP + FN} \tag{3-1}$$

where, true positive (TP) and false positive (FP) values represent the concordance pixels of background and foreground between predicted image and original image; and false negative (FN) values represent the disagreement between predicted image and original image.
The evaluation was done with the comparison of two CNN ensemble versions of SEUNet against UNet, SEUNet, DRIU, Pix2Pix as baseline models. We explored the original UNet, the UNet with SE-Blocks termed as SEUNet architecture. Besides, the original DRIU and the modified DRIU with SE-BLOCKS in the last layer to obtain a fine segmentation were tested.

The loss function for UNet and SEUNet was a binary cross-entropy plus Dice loss and, for DRIU architectures was used a binary cross-entropy plus the Jaccard as a unified loss function. These hyperparameters were founded by exploring in a grid search. The batch size and learning rate that obtained the lowest loss function in the first experiment with 50 epochs were chosen to increase the number of epochs. According to the best performance reported in tests for UNet, SEUNet, and DRIU, the models were trained using 450 epochs, a batch size of 16 images and a learning rate of 0.003 with Adam optimizer The Figure **3-3** shows the loss and performance metric values, during training for SEUNET method.

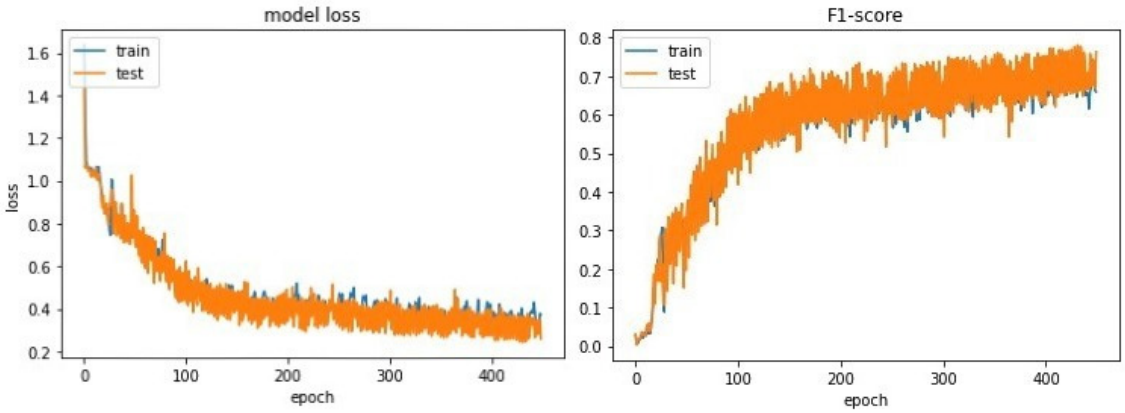


**Figure 3-3**: Loss and Dice performance train(blue) and validation (orange).

## 3.3 Results

The best models used in training and validation sets after exploring hyperparameters in a grid search were evaluated on the test set. The Dice coefficient obtained for retinal fluids and HFs segmentation tasks in validation and test sets is presented in Table **3-1**, DICE coefficient on test and validation sets of fluids and HFs, it was compared over architectures like: UNet, SEUNet, DRIU, and Pix2Pix, those networks, results for our method are in general for HFs better than other models showing a test and validation dice measure of 0,6935 and 0,4437, for fluids SEUNet gives a really good performance, an ensemble with Pix2Pix architecture improve results on test dataset giving a dice of 0,6245.

Baseline models presented commonly fail on performing segmentation on small areas, those kinds of areas are presented at most HFs. However, the adding of squeeze and excitation blocks at the last layers of DRIU shows an improvement in segmentation results for HFs as shown in Figures **3-4** and **3-5**. These figures allow us to compare the obtained segmentations of baseline methods regarding the proposed ensemble method, those images show the dice coefficient per image meanwhile in Table **3-1** results show the mean dice coefficient for images in the respective dataset.

| | UNet | SEUNet | DRIU | Pix2Pix | ensemble Pix2Pix | ensemble DRIU |
|---|---|---|---|---|---|---|
| **Fluids** | | | | | | |
| Validation | 0,5672 | 0,7241 | 0,6509 | 0,4257 | 0,7205 | 0,7084 |
| Test | 0,5333 | 0,6236 | 0,5525 | 0,4352 | **0,6245** | 0,5972 |
| **Hyperreflective foci** | | | | | | |
| Validation | 0,5393 | 0,6835 | 0,6839 | 0,4070 | 0,6418 | 0,6935 |
| Test | 0,3756 | 0,4272 | 0,4385 | 0,3407 | 0,3800 | **0,4437** |

**Table 3-1**: Results comparison over models and data sets for retinal fluids and hyperreflective foci. In bold is the highest DICE coefficient for the test set.

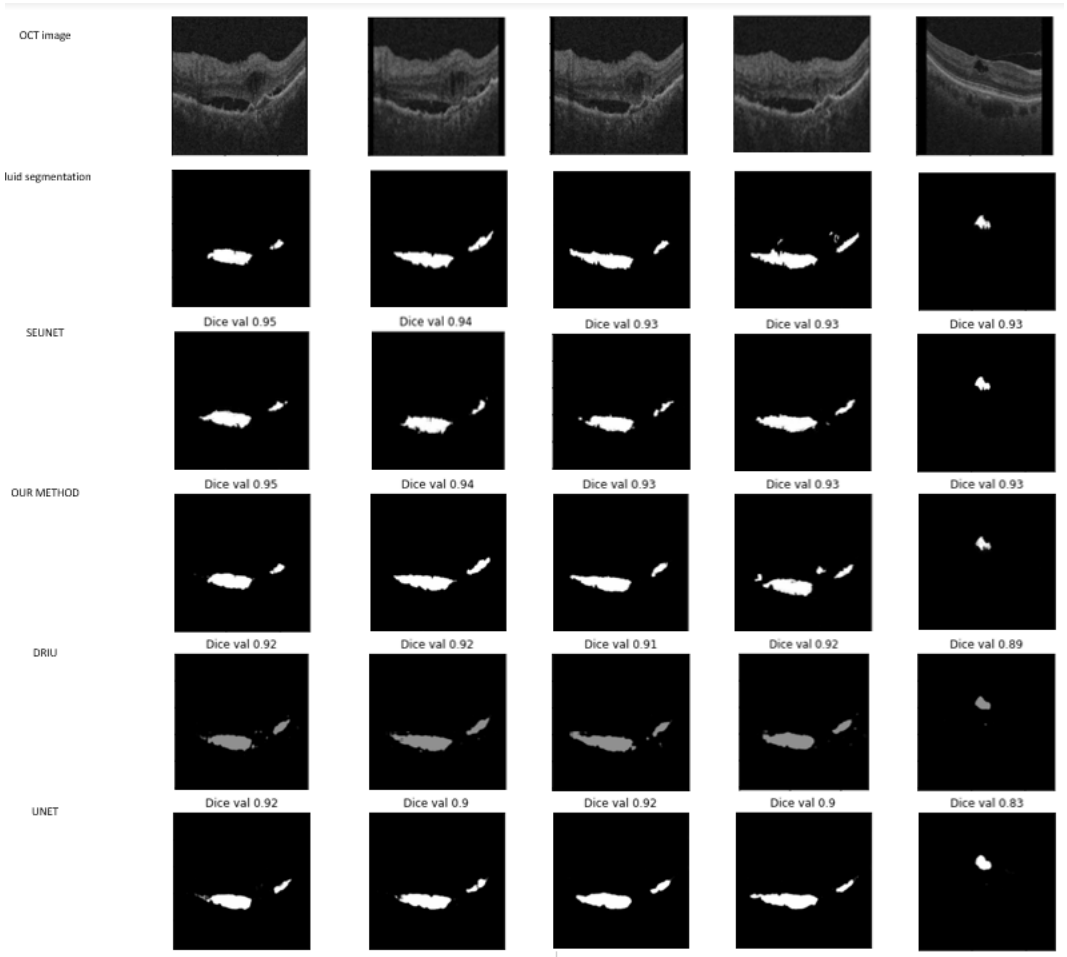


**Figure 3-4**: Fluid segmentation perform over dataset

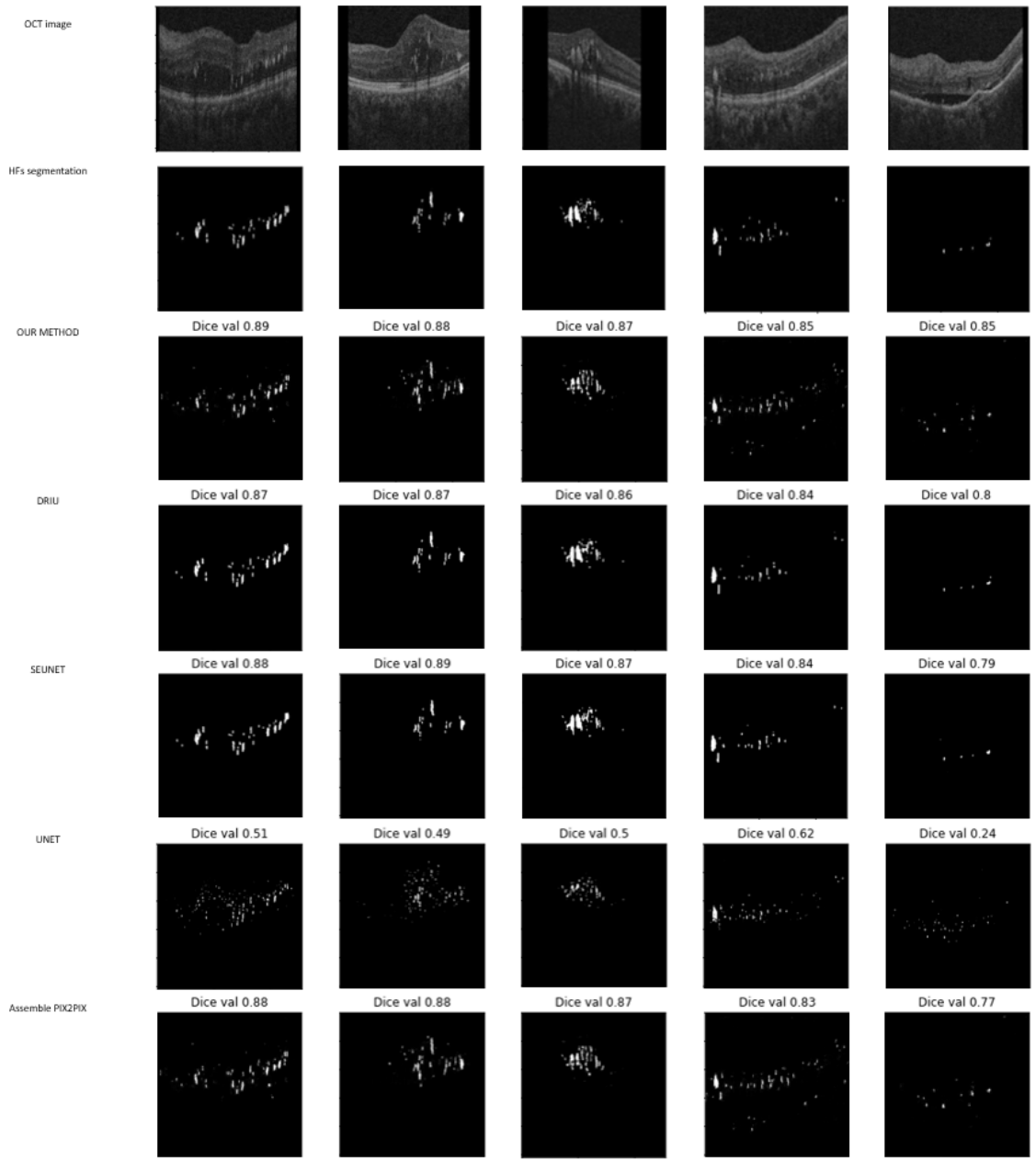


**Figure 3-5**: Hfs segmentation perform over dataset

## 3.4 Discussion and conclusions

Ophthalmologists guide their diagnosis according to the clinical findings found in scans. Thus, fluid and HFs segmentation plays an important role in eye disease classification-assisted diagnosis. This work provides an approach to automatically detect and segment

retinal fluids and HFs to support clinical decision-making in retinal diagnosis. This method reduces the time-consuming spend in the detection of findings and it could offer information about the fluid quantity in volumes.

HFs segmentation is a demanding time task even for experts because of small sizes and the closer presence to large retinal fluids of these findings. The obtained segmentation masks using the proposed ensembled model with Pix2Pix present the best results in HFs detection as reported in Table 1 and Figures 3-4. Otherwise, the baseline methods have a bad performance in most of the areas with a doted o very small segmentation region as normally present with HFs finding.

The method performance was compared with state-of-the-art methods, where our proposed method using the ensembled model of SEUNet with Pix2Pix presents the best results in the segmentation task of HFs and retinal fluid.

Other finding such as drusen may help to identify some diseases like retinal vein occlusion and vitreoretinal traction. However, datasets with drusen segmentation are still a need. The available datasets have bad quality and a reduced number of images. Moreover, the free public OCT data sets have no segmentation mask with ocular findings. In this work, we released a new image dataset with binary masks of retinal fluids and HFs available in two repositories [1] [2].

A major number of scans must be required to increase the significance of the obtained results. On the other hand, the segmentation of other findings will be studied in future works. Finally, we consider that the integration of this model with models to classify retinal disease could be used in screening programs to deliver additional relevant information to ophthalmologists.

[1] $https://github.com/yeisonlegarda/fluidsdukemarkeddataset.git$
[2] $https://github.com/yeisonlegarda/focisdukemarkeddataset.git$

# 4 Biomarker segmentation and Disease classification using a deep learning approach in optical coherence tomography scans

This chapter explores segmentation of different biomarkers such as fluids, HRFs, drusen, and cysts through the experimentation with OCT images, some state of art architectures were tested for this work, and also a proposed method based on a DRIU network modified, in addition to segmentation, binary and multiple classifications are also explored for labeled OCT scans; scans used for classification and segmentation were annotated by an expert ophthalmologist from the ophthalmology department of Universidad Nacional de Colombia.

## 4.1 Introduction

There is an upward trend of population aging and, consequently, a significant increase in the global burden of chronic diseases. Among these, the most representative ocular disorders are age-related macular degeneration (AMD), diabetic retinopathy (DR), and retinal vein occlusion (RVO).[69] These diseases converge in macular edema development, which is the most important cause of visual impairment due to structural and functional sequelae.[70] These exudative retinal diseases are responsible for most blindness cases that affect the macula both with the generation of edema and the development of an intense inflammatory response that accelerates the damage progression.[71][72].

Macular edema is the fluid accumulation or swelling that occurs in the retinal extracellular space in the macula, which is an important area located in the center of the retina and needed for sharp vision and fine detail, and color recognition. This build-up of fluid leads to abnormal macular thickening and represents an important cause of central vision loss.[70] Therefore, early detection of macular edema is critical for proper diagnosis and management to get better visual results.[70]

The structural and functional integrity of the retina is maintained by a state of relative dehydration that ensures its transparency and optimal transmission of light to the photoreceptors. The accumulation of fluid in the intra and subretinal regions results from the loss

of balance of the active and passive mechanisms that govern the entry and exit of fluid, as represented by the Starling equation when a pathological condition interrupts the integrity of the blood-retinal barrier. It is composed of both an inner and an outer barrier. The inner one comprises the vascular endothelium, basement membrane, and pericytes, and the outer one is made up of the retinal pigment epithelium.[70][73].

The pathogenesis of diabetic macular edema includes a hyperglycemic state that causes tissue damage through oxidative stress, advanced glycation end products, blood flow impairment, hypoxia, pericytes, and endothelial cells loss, inflammation, and decrease of neural protective factors such as glial cell line-derived neurotrophic factor.[74][75] In cases of retinal vein occlusion, the formation of macular edema results from the cytokine release, hypoxia, and increased hydrostatic pressure and vascular stasis leading to the subsequent interstitial fluid accumulation, according to Starling equation.[76][77]

The choroidal neovascular membranes related to wet age-related macular degeneration conduce to fluid accumulation in the macular area due to disruption of the retinal pigment epithelium (outer blood-retinal barrier), with the amplification of endothelial damage and increased vascular permeability by proinflammatory cytokines, hypoxia, pro-angiogenic molecules and oxidative stress (breakdown of the inner blood-retinal barrier).[72][78].

The differentiation of macular edema etiology is of vital importance for the recognition of visual prognosis and the most suitable therapeutic approach. Optical coherence tomography (OCT) is the method of choice for studying macular edema.[70] it allows the best evaluation by recognizing the proper location, extension, and significant disease patterns that are so helpful to determine the underlying pathology.[79]

The most representative patterns of diagnostic images are capable of being identified, processed, and quantified. These findings are known as biomarkers, which are certain characteristics that can be objectively measured and evaluated as indicators of normal or pathological biological processes, with their respective diagnostic, predictive and prognostic values.[80],[81].

Macular edema due to choroidal neovascular membrane secondary to wet age-related macular degeneration exhibits distinctive biomarkers such as drusen, hyperreflective foci, drusenoid pigment epithelial detachment (PED) and subretinal fluid.[82][**?**]. Diabetic macular edema shows disorganization of retinal inner layers (DRIL), epiretinal membrane, intraretinal fluid, and hyperreflective foci.[83][84]. Macular edema due to retinal vein occlusion reveals typical biomarkers like retinal macrocysts, hyperreflective foci, subretinal fluid, and outer limiting membrane disruption.[85][37].

The growing incidence of the above-mentioned age-related ocular diseases increases the number of office visits, regular specialized check-ups, treatment sessions, and diagnostic tests, which are much higher than the number of expert specialists who can analyze them promptly. As a comprehensive strategy to overcome these needs there is digital health, and among its strategies, the application of artificial intelligence arises to support diagnosis, access, and timely reading of diagnostic images.

Many challenges exist in working with OCT images and machine learning, these include data

availability because legal reasons and privacy make it impossible to share data information with which the methods were trained and tested, OCT images also have some singularities such as highly noisy foreground and background textures are quite similar, images between different vendors have too many differences in appearance and features, doing for an automated method harder to perform generalization over these kinds of images, mostly of times this problem is tackled by adding stages of pre-processing and post-processing but and although additional steps don't limit the usability of the methods, they do require domain knowledge; at last biomarkers, segmentation is hard due to the different sizes, shapes and location that these have.

In this work, an automated end-to-end system based on a deep learning algorithm is proposed to automatically perform the segmentation of biomarkers ( drusen, HRF, fluids, and cyst) and classification of diseases having into account the results from segmentation performed on OCT images. The remainder of the article is organized as follows: Section 4.2 explains in detail the proposed method, dataset, and evaluation. Section 3.3 shows the experimental results obtained in the segmentation task. Finally, section 4.4 reports the main discussion, conclusions and future works.

## 4.2 Methodology

### 4.2.1 Dataset

The scans were manually annotated with biomarkers by an expert ophthalmologist; biomarkers include fluids(IRF, SRF), HRF, cyst, and drusen; expert ophthalmologist also labeled each OCT scan with disease (AMD, DME, RVO) for cases where the disease could be seen in the scan if scan image hasn't got any disease this was labeled as control, a total of 1343 images were annotated, these images were divided into seven different datasets four of which belongs to biomarkers segmentation and the rest belonging to diseases, datasets were balanced to get the same proportion of images in segmentation case between images with findings and those without any finding, similarly was done for diseases wit healthy images and images where the disease could be seen. After having balanced datasets each one is partitioned between training, test, and validation containing 70%,20% and 10% of total images respectively the total images pet set are related in Table **4-1**.

| Segmentation | | | | |
|---|---|---|---|---|
| | **Training** | **Test** | **Validation** | **Total** |
| **Drusen** | 498 | 146 | 70 | 714 |
| **HRF** | 486 | 141 | 68 | 695 |
| **Fluids** | 242 | 70 | 34 | 346 |
| **Cyst** | 250 | 74 | 34 | 360 |
| **Classification** | | | | |
| **AMD** | 154 | 46 | 22 | 222 |
| **RVO** | 244 | 72 | 34 | 350 |
| **DME** | 26 | 9 | 3 | 38 |

**Table 4-1**: Images per dataset resume for image classification and segmentation on OCT scans

### 4.2.2 Deep learning method

The overall pipeline for the segment and classify OCT images are shown in figure **4-1**, this includes the first step for segment cyst, drusen, HRF, and fluids, a second step includes classify the image between three diseases these include AMD, DME, and RVO.

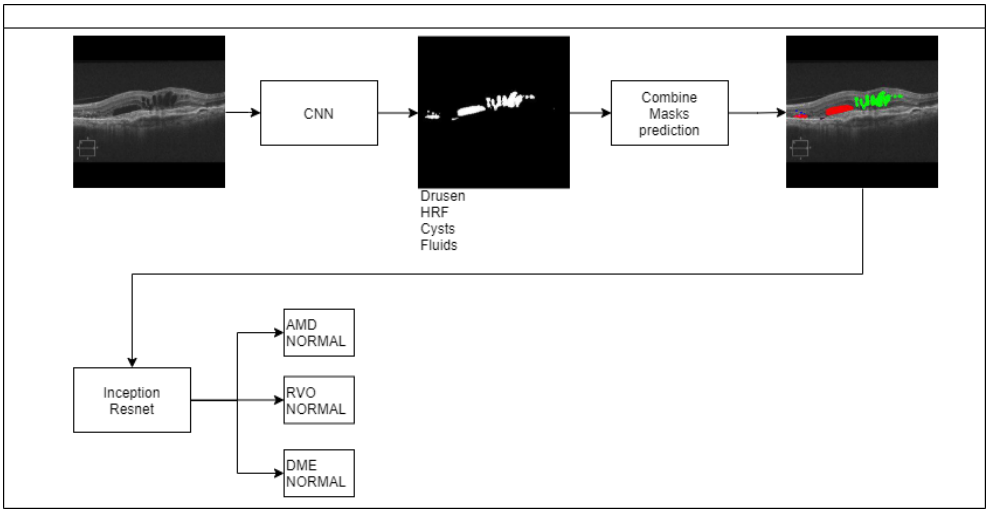


**Figure 4-1**: Block diagram of the proposed method to classify and segment OCT images.

#### OCT scans segmentation

For image segmentation two architectures there were used: ResUNet++[86] this is an architecture based on ResUNet which is a UNET architecture with residual blocks on it, those

residual units allow to learn the residual functions between inputs and outputs not only the mapping of those ones[35], on ResUNet++ squeeze-and-excitation (SE) blocks are added on encoder path after each block [86], SE has shown to be a point of improvement for CNNs by replacing some of the network components with its equivalent to SE, the result its a SENet which allows to increases the sensitivity of the network to relevant features and suppress irrelevant ones through the use of two operations squeeze that refers to global spatial information embedding into a channel description equation 4-1 [87] shows the squeeze operation based on global average pooling.

$$Z_c = \frac{1}{H \times W} \sum_{i=1}^{H} \sum_{j=1}^{W} U_c(i,j) \tag{4-1}$$

where $H$ is the height and $W$ the weight of the input tensor and $U_c$ the c-the feature map of the input. After squeeze operation comes excitation operation [**?**] [87] made for getting channel-wise dependencies, this can be achieved by employing a sigmoid activation.

$$s = \sigma(W_2 \delta(W_1 z)) \tag{4-2}$$

where $W_1$ and $W_2$ denote the fully connected operation $\delta$ refers to RELU operation and $\sigma$ the sigmoid operation.

Lastly, a rescaling of feature map with activation $s$ its performed equation 4-3 [87] shows the operation which it's a channel-wise multiplication.

$$\bar{X} = S_c U_c \tag{4-3}$$

where $\bar{X}$ is the SE operation output, $S_c$ and $U_c$ the scalar and the feature map respectively.

For segmentation also was used a DRIU architecture based on VGG-19 was used for the segmentation of optic disc and blood vessels in eye fundus images[65], some changes were performed on this architecture, the first one was adding batch normalization layers to improve the training speed and training convergence also the batch normalization layer can improve the network generalization ability[52] another change was adding ES blocks on last layers of the network, figure **4-2**shows the network architecture used.

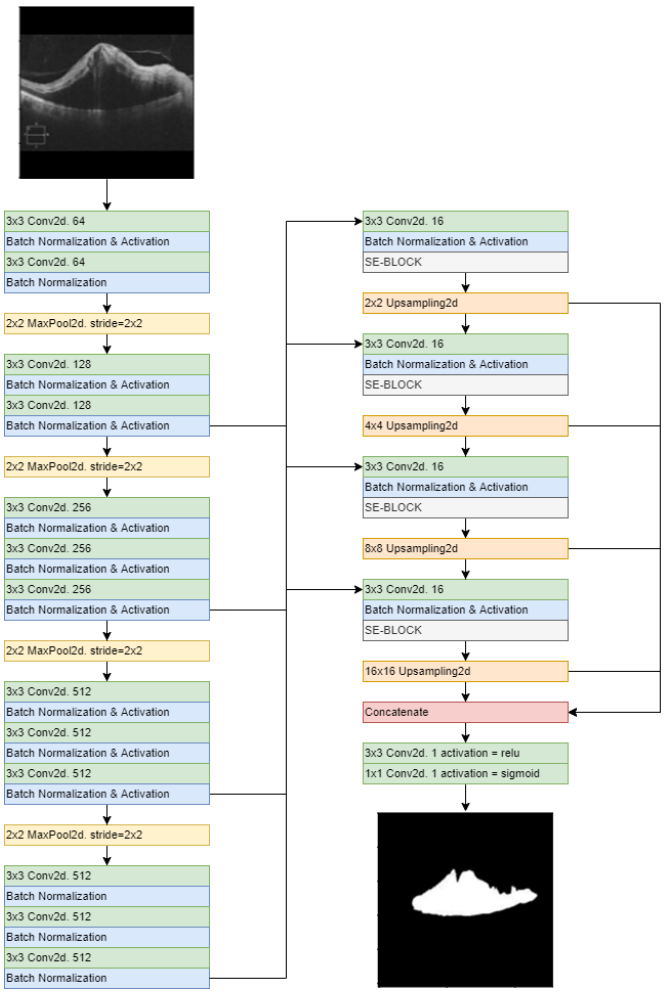


**Figure 4-2**: Modified DRIU architecture for biomarkers segmentation in OCT scans

For segmentation, training images are normalized, and data augmentation is performed, operations for data augmentation include flip and random crops over images.

### OCT scans classification

Classification over scans is performed with two approaches first one was taking the single scan and the second one was taking the scan and passing through models for segment fluid, cyst, and HRF placing each prediction on an image channel respectively, for drusen a linear combination of data prediction was made on the first and third channel of resulting image after staking predictions of fluid, cyst and HRF, the resulting image of previous operations it's superimposed on the original image, figure show image for the first and second approach.

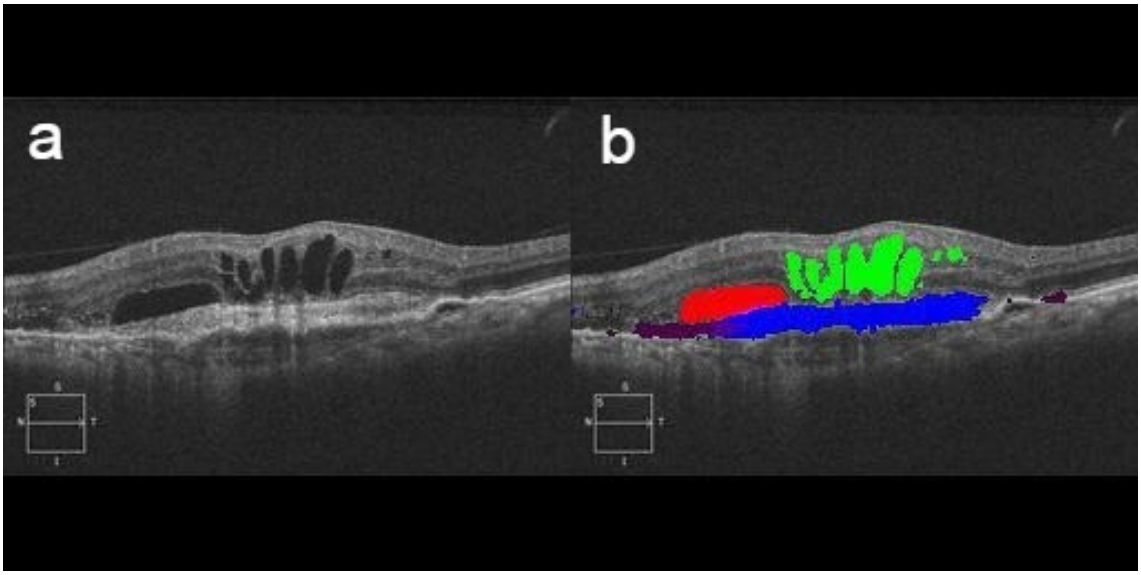


**Figure 4-3**: a) Single Scan , b) Scan with fluids (red),cyst(green), HRF (blue) and drusen (purple) predicted by models.

Scans for classification both cases (single scan, scan with predictions), are normalized and also to perform data augmentation operations like horizontal flip, zooming, and cropping, after operations an Inception-ResNet-v2 architecture is used for training the classification model, Inception-ResNet-v2 architecture uses residual connections version for Inception-v4 network[ChristianSzegedy2016]. To verify both classifications approaches DUKE dataset [46] was used, this dataset contains 269 volumes for AMD patients and 115 control volumes each volume contains 100 images, to use this dataset due to noise of images BM3D algorithm with a sigma value of 12 it was used for denoising, after denoising images the classifications models were applied with a voting strategy to classify each volume between control and AMD, for voting strategy was defined a threshold given by the average of AMD OCT slices predicted on control volumes then if a volume has several slices marked as AMD less than the average, the volume is considered as a normal subject.

## 4.3 Results

### 4.3.1 Evaluation

To evaluate the network's architecture was used dice coefficient shown in equation 4-4 this is a performance metric that measures the pixel's overlap between two images, allowing to look up for the similarity between ground truth and segmentation provided by models [8].

$$\text{DSC} = \frac{2\text{TP}}{2\text{TP} + \text{FP} + \text{FN}} \tag{4-4}$$

In equation 4-4 TP is true positive pixels, FP false positive pixels, and FN false negative pixels after comparing ground truth with segmentation results.
For scans classification were used the following performance metrics: accuracy, sensitivity and specificity shown in equations 4-5 4-6 4-7 respectively. [29][20]

$$\text{Accuracy} = \frac{\text{TP} + \text{TN}}{\text{TP} + \text{TN} + \text{FP} + \text{FN}} \tag{4-5}$$

$$\text{Sensitivity} = \frac{\text{TP}}{\text{TP} + \text{FN}} \tag{4-6}$$

$$\text{Specificity} = \frac{\text{TN}}{\text{TN} + \text{FP}} \tag{4-7}$$

### 4.3.2 Results

#### Scans segmentation

Table **4-2** shows the results for OCT scans segmentation we compare the proposed architectures with state of the art architectures, as can be seen our method achieves best results for fluid segmentation and comparable results with model which obtains best result for three of four segmented biomarkers, this is RESUNET++, however for training and prediction proposed method has got a better performance this takes 40 minutes and a second to training and predict a single scan respectively, whereas RESUNET++ takes 1 hour and 2 seconds for training and predict single OCT scan respectively, training for both methods were performed for 200 epochs, in images **4-4**,**4-5**,**4-6** and **4-7** segmentation for OCT slices in test dataset are shown respectively, those segmentation are the result of manual segmentation performed by the expert ophthalmologist and automatic segmentation performed by the RESUNET++ and proposed method.

| | **Fluids** | | **HRF** | | **Cyst** | | **Drusen** | |
|---|---|---|---|---|---|---|---|---|
| | **Validation** | **Test** | **Validation** | **Test** | **Validation** | **Test** | **Validation** | **Test** |
| RESUNET++ | 0.6650 | 0.6213 | 0.5728 | **0.5686** | 0.8269 | **0.8211** | 0.6346 | **0.6037** |
| Proposed | 0.6968 | **0.6657** | 0.5834 | 0.5432 | 0.8183 | 0.8000 | 0.6806 | 0.5973 |
| SEUNET | 0.6639 | 0.6594 | 0.5344 | 0.4537 | 0.8321 | 0.7200 | 0.5967 | 0.5269 |
| DRIU | 0.6508 | 0.6213 | 0.5369 | 0.5209 | 0.8151 | 0.7877 | 0.6646 | 0.5291 |

**Table 4-2**: Dice coefficient for biomarkers segmentation over tested architectures

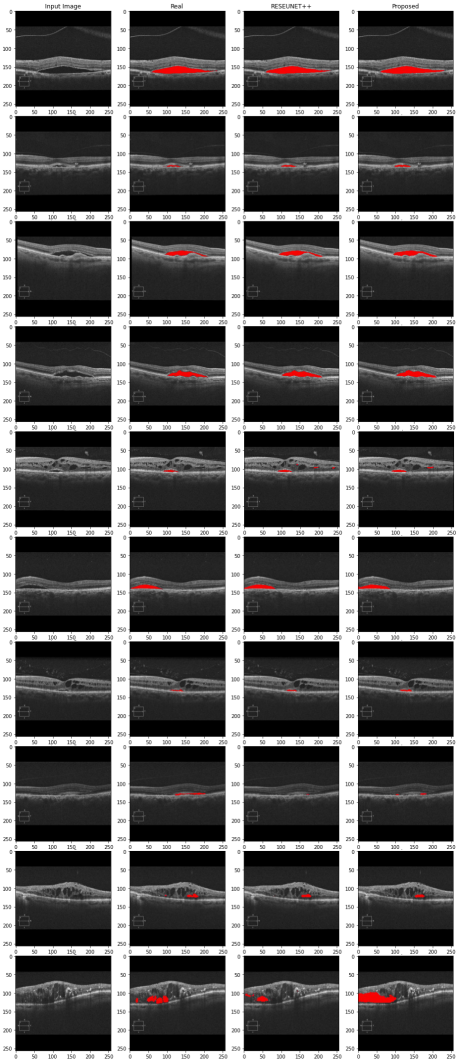


**Figure 4-4**: Fluid segmentation performed by expert ophthalmologist, RESUNET++ and proposed method over different OCT scans

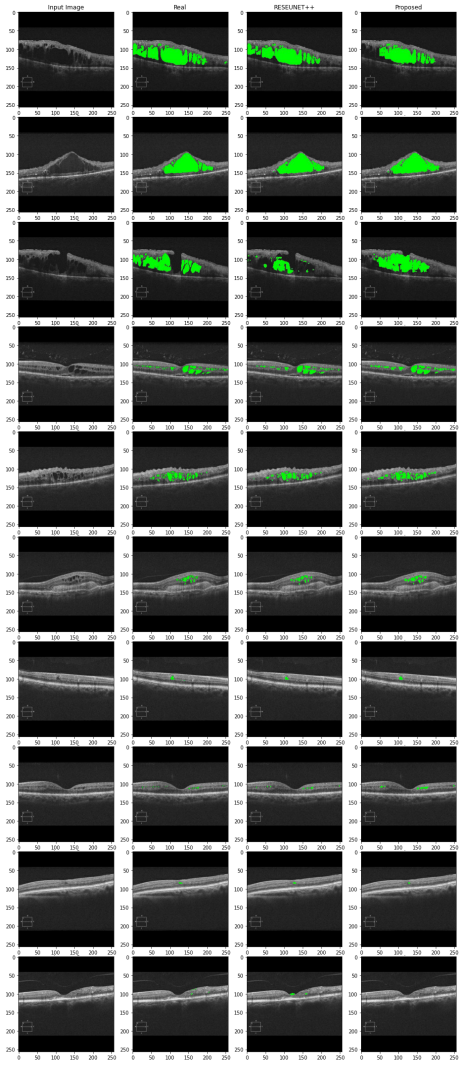


**Figure 4-5**: Cyst segmentation performed by expert ophthalmologist, RESUNET++ and proposed method over different OCT scans

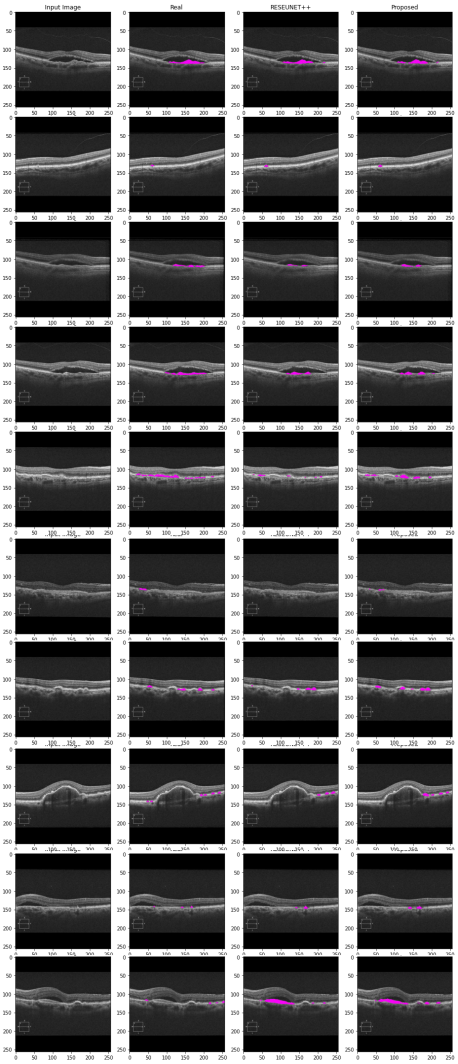


**Figure 4-6**: Drusen segmentation performed by expert ophthalmologist, RESUNET++ and proposed method over different OCT scans

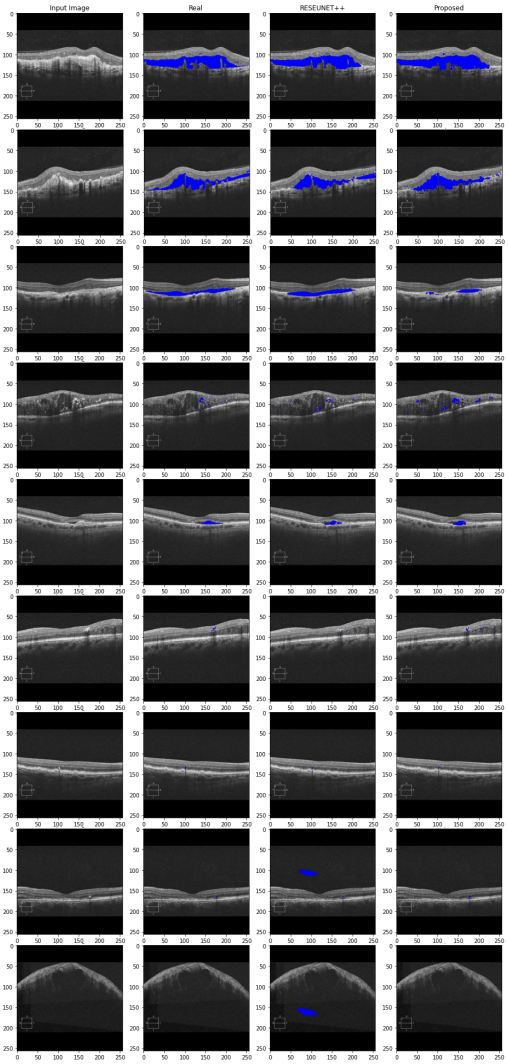


**Figure 4-7**: HRFs segmentation performed by expert ophthalmologist, RESUNET++ and proposed method over different OCT scans

### Scans classification

Oct scan classifications were made with Inception-ResNet-v2 but with different approaches in images as was already explained, in the image including segmentation case were taken images from results of the proposed method and RESUNET++, tables **4-3** and **4-4** show metrics results for AMD and RVO classification respectively, as can be seen, the best results are achieved by the image with segmentation information for the proposed method in AMD case, for RVO results are better for images with segmentation don't matter the method used for segmentation.

| | Validation | | | | Test | | | |
|---|---|---|---|---|---|---|---|---|
| | **Accuracy** | **Precision** | **Recall** | **F1-Score** | **Accuracy** | **Precision** | **Recall** | **F1-Score** |
| **Scan + proposed segmentation** | 1 | 1 | 1 | 1 | 1 | 1 | 1 | 1 |
| **Scan + RESUNET++ segmentation** | 1 | 1 | 1 | 1 | 0.9783 | 0.9791 | 0.9783 | 0.9783 |
| **Single scan** | 1 | 1 | 1 | 1 | 0.9783 | 0.9791 | 0.9783 | 0.9783 |

**Table 4-3**: Classification results for AMD

| | Validation | | | | Test | | | |
|---|---|---|---|---|---|---|---|---|
| | Accuracy | Precision | Recall | F1-Score | Accuracy | Precision | Recall | F1-Score |
| Scan + proposed segmentation} | 1 | 1 | 1 | 1 | 0.9583 | 0.9615 | 0.9583 | 0.9583 |
| Scan + RESUNET++ segmentation | 1 | 1 | 1 | 1 | 0.9583 | 0.9615 | 0.9583 | 0.9583 |
| Single scan | 1 | 1 | 1 | 1 | 0.9583 | 0.9586 | 0.9583 | 0.9583 |

**Table 4-4**: Classification results for RVO

Table **4-5** shows the classification performance for duke dataset.

| | **Accuracy** | **Sensitivity** | **Specificity** |
|---|---|---|---|
| **Single scan** | 0.8142 | 0.6633 | 0.9144 |
| **Scan + proposed method** | 0.7035 | 0.68 | 0.7171 |
| **Scan + RESUNET++** | 0.7430 | 0.7128 | 0.7631 |

**Table 4-5**: Classification results for AMD on DUKE dataset using voting strategy

## 4.4 Conclusions and discussions

This paper proposes an end-to-end method applied to OCT scans for the automatic segmentation of biomarkers and classification of macular diseases, for the segmentation task were explored two CNN architectures, the first one based on integrating SE blocks and BN layers to a DRIU architecture, and the second one making use of RESUNET++ architecture. The RESUNET++ method performs good results on foci, cyst, and drusen with a dice coefficient in the test set of 0.5686,0.8211, and 0.6037, respectively for fluids case our method shows the best performance with a test dice of 0.6657. However, when performing segmentation RESUNET++ adds false positive pixels on outside retinal layers as can be seen in figures **4-5** and **4-7** which belongs to segmentation for fluids and cysts. The proposed method achieves the state-of-the-art performance for segmentation architectures, showing an improvement over the original architecture (DRIU) for OCT scans segmentation.
For the classification of macular diseases using OCT scans, two approaches were explored. An Inception-ResNet-v2 with the raw scan as an input and the second approach that combines

the raw OCT scans with the generated segmentation performed by the proposed method and RESUNET++. Best results are shown by scans without segmentation information; however, for DME case, very few images are available, so the results may not be generalizable; for posterior works, more images should be added to DME class, and also other architectures may be explored comparing their results to look for a performance boost for all classification cases.

At last for developing this work, hyperparameter tuning presented a significant challenge because the quality of results depends mainly on the hyperparameters used for training, then two hyperparameter tuning ways were tested random search and also a grid search, best performance presented was to random search for which the results obtained for both classification and segmentation were presented.

The wide variety of vendors for OCT scans is still a problem to be addressed. For this work, an existing marked with AMD dataset was used for classification using the pre-trained network with our dataset; nevertheless, a preprocessing algorithm should be applied to achieve good results. For future works, an end-to-end method can be explored to avoid such discrepancies between vendors.

# 5 Conclusion and future works

This research explored several deep learning approaches to automatically obtain the image segmentation of macular biomarkers using OCT scans. However, the segmentation of these macular biomarkers is not an easy task due to the different shapes, sizes, and textures of the analyzed biomarkers (HRFs, Fluids, Drusen, Cyst). To tackle this problem a deep learning architecture known as DRIU was modified with elements that have shown pretty good performance by increasing results over some architectures, the proposed method shows comparable results with state-of-the-art methods.

In addition, the classification of OCT scans between different macular diseases was explored in this thesis. Two approaches were taken into account single images classification and images predicted from segmentation models for all biomarkers, an architecture name inception Resnet-v2 was chosen for this task, the results after hyperparameter exploration, show that images with annotated biomarkers do not provide comparable results with single images, then for binary classification better to give to network architecture images without extra information, in addition to the binary classification in this research the multiclassification problem was addressed by making use of the same architecture employed for binary classification, this was possible due to data availability provided by the Departamento de oftalmología from Universidad Nacional de Colombia because no public datasets provide annotated scans with all diseases, this was also the case for OCT scans segmentation.

The obtained results were validated through comparison with the state-of-the-art methods, because in most cases the images used in the state of the art methods couldn't be obtained, due to data privacy or because some public datasets didn't possess all biomarkers or diseases to be tackled; the results obtained show that proposed methods for classification and segmentation are comparable to state of art methods.

Finally, some open challenges are still latent, i.e. a strategy to segment and classify OCT scans from multi-ophthalmology centers, this is the most remarkable challenge because of the scans differences such as size and quality in this research the way to tackle this problem was through image denoising but other ways must be explored. Another possible future work may be the automatic generation of artificial OCT scans with no common ocular findings or diseases, due to the amount of data needed to get good results in commonly used approaches.

# Bibliography


[1] J D Moura, J Novo, and M Ortega. Deep Feature Analysis in a Transfer Learning-based Approach for the Automatic Identification of Diabetic Macular Edema. In *Proceedings of the International Joint Conference on Neural Networks*, volume 2019-July, 2019.

[2] B Hassan, T Hassan, B Li, R Ahmed, and O Hassan. Deep ensemble learning based objective grading of macular edema by extracting clinically significant findings from fused retinal imaging modalities. *Sensors (Switzerland)*, 19(13), 2019.

[3] Z Xu, W Wang, J Yang, J Zhao, D Ding, F He, D Chen, Z Yang, X Li, W Yu, and Y Chen. Automated diagnoses of age-related macular degeneration and polypoidal choroidal vasculopathy using bi-modal deep convolutional neural networks. *British Journal of Ophthalmology*, 105(4):561–566, 2021.

[4] M R Ibrahim, K M Fathalla, and S M Youssef. HyCAD-OCT: A hybrid computer-aided diagnosis of retinopathy by optical coherence tomography integrating machine learning and feature maps localization. *Applied Sciences (Switzerland)*, 10(14), 2020.

[5] A Adel, M M Soliman, N E M Khalifa, and K Mostafa. Automatic Classification of Retinal Eye Diseases from Optical Coherence Tomography using Transfer Learning. In *16th International Computer Engineering Conference, ICENCO 2020*, pages 37–42, 2020.

[6] Varun Gulshan, Lily Peng, Marc Coram, Martin C Stumpe, Derek Wu, Arunachalam Narayanaswamy, Subhashini Venugopalan, Kasumi Widner, Tom Madams, Jorge Cuadros, and Others. Development and validation of a deep learning algorithm for detection of diabetic retinopathy in retinal fundus photographs. *Jama*, 316(22):2402–2410, 2016.

[7] Freerk G Venhuizen, Bram van Ginneken, Bart Liefers, Freekje van Asten, Vivian Schreur, Sascha Fauser, Carel Hoyng, Thomas Theelen, and Clara I Sánchez. Deep learning approach for the detection and quantification of intraretinal cystoid fluid in multivendor optical coherence tomography. *Biomedical Optics Express*, 9(4):1545–1569, 2018.

[8] Behnam Azimi, Abdolreza Rashno, and Sadegh Fadaei. Fully Convolutional Networks for Fluid Segmentation in Retina Images. In *2020 International Conference on Machine Vision and Image Processing (MVIP)*, pages 1–7, 2020.

[9] Xiaoming Liu, Shaocheng Wang, Ying Zhang, Dong Liu, and Wei Hu. Automatic fluid segmentation in retinal optical coherence tomography images using attention based deep learning. *Neurocomputing*, 452:576–591, 2021.

[10] Karthik Gopinath and Jayanthi Sivaswamy. Domain knowledge assisted cyst segmentation in OCT retinal images. *CoRR*, abs/1612.0, 2016.

[11] Shekoufeh Gorgi Zadeh, Maximilian W M Wintergerst, Vitalis Wiens, Sarah Thiele, Frank G Holz, Robert P Finger, and Thomas Schultz. CNNs Enable Accurate and Fast Segmentation of Drusen in Optical Coherence Tomography BT - Deep Learning in Medical Image Analysis and Multimodal Learning for Clinical Decision Support. pages 65–73, Cham, 2017. Springer International Publishing.

[12] Sha Xie, Idowu Paul Okuwobi, Mingchao Li, Yuhan Zhang, Songtao Yuan, and Qiang Chen. Fast and Automated Hyperreflective Foci Segmentation Based on Image Enhancement and Improved 3D U-Net in SD-OCT Volumes with Diabetic Retinopathy. *Translational Vision Science  Technology*, 9(2):21, apr 2020.

[13] Thomas Schlegl, Philipp Seeböck, Sebastian M Waldstein, Ursula Schmidt-Erfurth, and Georg Langs. Unsupervised anomaly detection with generative adversarial networks to guide marker discovery. In *International conference on information processing in medical imaging*, pages 146–157. Springer, 2017.

[14] László Varga, Attila Kovács, Tamás Grósz, Géza Thury, Flóra Hadarits, Rózsa Dégi, and József Dombi. Automatic segmentation of hyperreflective foci in OCT images. *Computer Methods and Programs in Biomedicine*, 178:91–103, 2019.

[15] Ruwan Tennakoon, Amirali K Gostar, Reza Hoseinnezhad, and Alireza Bab-Hadiashar. Retinal fluid segmentation in OCT images using adversarial loss based convolutional neural networks. In *2018 IEEE 15th International Symposium on Biomedical Imaging (ISBI 2018)*, pages 1436–1440, 2018.

[16] Abdolreza Rashno, Behzad Nazari, Dara D Koozekanani, Paul M Drayna, Saeed Sadri, Hossein Rabbani, and Keshab K Parhi. Fully-automated segmentation of fluid regions in exudative age-related macular degeneration subjects: Kernel graph cut in neutrosophic domain. *PLOS ONE*, 12(10):1–26, 2017.

[17] Xiaoming Liu, Dong Liu, Bo Li, and Shaocheng Wang. Deep learning based fluid segmentation in retinal optical coherence tomography images. In *International Conference on Intelligent Computing*, pages 337–345. Springer, 2019.

[18] Shekoufeh Gorgi Zadeh, Maximilian W M Wintergerst, and Thomas Schultz. Intelligent interaction and uncertainty visualization for efficient drusen and retinal layer segmentation in Optical Coherence Tomography. *Computers  Graphics*, 83:51–61, 2019.

[19] Rui Zhao, Acner Camino, Jie Wang, Ahmed M Hagag, Yansha Lu, Steven T Bailey, Christina J Flaxel, Thomas S Hwang, David Huang, Dengwang Li, and Yali Jia. Automated drusen detection in dry age-related macular degeneration by multiple-depth, en face optical coherence tomography. *Biomedical Optics Express*, 8(11):5049–5064, 2017.

[20] Zailiang Chen, Dabao Li, Hailan Shen, Hailan Mo, Ziyang Zeng, and Hao Wei. Automated segmentation of fluid regions in optical coherence tomography B-scan images of age-related macular degeneration. *Optics  Laser Technology*, 122:105830, 2020.

[21] Philipp Seeböck, David Romo-Bucheli, Sebastian Waldstein, Hrvoje Bogunovic, José Ignacio Orlando, Bianca S Gerendas, Georg Langs, and Ursula Schmidt-Erfurth. Using Cyclegans for Effectively Reducing Image Variability Across OCT Devices and Improving Retinal Fluid Segmentation. In *2019 IEEE 16th International Symposium on Biomedical Imaging (ISBI 2019)*, pages 605–609, 2019.

[22] Timothy R Fricke, Nina Tahhan, Serge Resnikoff, Eric Papas, Anthea Burnett, Suit May Ho, Thomas Naduvilath, and Kovin S Naidoo. Global prevalence of presbyopia and vision impairment from uncorrected presbyopia: systematic review, meta-analysis, and modelling. *Ophthalmology*, 125(10):1492–1499, 2018.

[23] Wen Liu, Yankui Sun, and Qingge Ji. MDAN-UNet: Multi-Scale and Dual Attention Enhanced Nested U-Net Architecture for Segmentation of Optical Coherence Tomography Images, 2020.

[24] N Motozawa, G An, S Takagi, S Kitahata, M Mandai, Y Hirami, H Yokota, M Akiba, A Tsujikawa, M Takahashi, and Y Kurimoto. Optical Coherence Tomography-Based Deep-Learning Models for Classifying Normal and Age-Related Macular Degeneration and Exudative and Non-Exudative Age-Related Macular Degeneration Changes. *Ophthalmology and Therapy*, 8(4):527–539, 2019.

[25] Who. Vision impairment and blindness, 2021.

[26] Soichiro Kuwayama, Yuji Ayatsuka, Daisuke Yanagisono, Takaki Uta, Hideaki Usui, Aki Kato, Noriaki Takase, Yuichiro Ogura, and Tsutomu Yasukawa. Automated detection of macular diseases by optical coherence tomography and artificial intelligence machine learning of optical coherence tomography images. *Journal of ophthalmology*, 2019, 2019.

[27] I Oguz, L Zhang, M D Abràmoff, and M Sonka. Optimal retinal cyst segmentation from OCT images. In *Progress in Biomedical Optics and Imaging - Proceedings of SPIE*, volume 9784, 2016.

[28] Zubin Mishra, Anushika Ganegoda, Jane Selicha, Ziyuan Wang, SriniVas R Sadda, and Zhihong Hu. Automated Retinal Layer Segmentation Using Graph-based Algorithm Incorporating Deep-learning-derived Information. *Scientific Reports*, 10(1):9541, 2020.

[29] V Rajinikanth, R Sivakumar, D J Hemanth, S Kadry, J R Mohanty, S Arunmozhi, N S M Raja, and N G Nhu. Automated classification of retinal images into AMD/non-AMD Class—a study using multi-threshold and Gassian-filter enhanced images. *Evolutionary Intelligence*, 2021.

[30] Samina Khalid, M Usman Akram, Taimur Hassan, Amina Jameel, and Tehmina Khalil. Automated Segmentation and Quantification of Drusen in Fundus and Optical Coherence Tomography Images for Detection of ARMD. *Journal of Digital Imaging*, 31(4):464–476, 2018.

[31] M Treder, J L Lauermann, and N Eter. Automated detection of exudative age-related macular degeneration in spectral domain optical coherence tomography using deep learning. *Graefe's Archive for Clinical and Experimental Ophthalmology*, 256(2):259–265, 2018.

[32] A Serener and S Serte. Dry and wet age-related macular degeneration classification using OCT images and deep learning. In *2019 Scientific Meeting on Electrical-Electronics and Biomedical Engineering and Computer Science, EBBT 2019*, 2019.

[33] Ali Mohammad Alqudah. AOCT-NET: a convolutional network automated classification of multiclass retinal diseases using spectral-domain optical coherence tomography images. *Medical Biological Engineering Computing*, 58(1):41–53, 2020.

[34] Daisuke Nagasato, Hitoshi Tabuchi, Hiroki Masumoto, Hiroki Enno, Naofumi Ishitobi, Masahiro Kameoka, Masanori Niki, and Yoshinori Mitamura. Automated detection of a nonperfusion area caused by retinal vein occlusion in optical coherence tomography angiography images using deep learning. *PLOS ONE*, 14(11):e0223965, nov 2019.

[35] Thomas Schlegl, Sebastian M Waldstein, Hrvoje Bogunovic, Franz Endstraßer, Amir Sadeghipour, Ana-Maria Philip, Dominika Podkowinski, Bianca S Gerendas, Georg Langs, and Ursula Schmidt-Erfurth. Fully Automated Detection and Quantification of Macular Fluid in OCT Using Deep Learning. *Ophthalmology*, 125(4):549–558, 2018.

[36] Melinda Katona, Attila Kovács, László Varga, Tamás Grósz, József Dombi, Rózsa Dégi, and László G Nyúl. Automatic detection and characterization of biomarkers in OCT images. In *International Conference Image Analysis and Recognition*, pages 706–714. Springer, 2018.

[37] Chenchen Yu, Sha Xie, Sijie Niu, Zexuan Ji, Wen Fan, Songtao Yuan, Qinghuai Liu, and Qiang Chen. Hyper-reflective foci segmentation in SD-OCT retinal images with diabetic

retinopathy using deep convolutional neural networks. *Medical Physics*, 46(10):4502–4519, oct 2019.

[38] Gabriella Moraes, Dun Jack Fu, Marc Wilson, Hagar Khalid, Siegfried K Wagner, Edward Korot, Daniel Ferraz, Livia Faes, Christopher J Kelly, Terry Spitz, Praveen J Patel, Konstantinos Balaskas, Tiarnan D L Keenan, Pearse A Keane, and Reena Chopra. Quantitative Analysis of OCT for Neovascular Age-Related Macular Degeneration Using Deep Learning. *Ophthalmology*, 128(5):693–705, 2021.

[39] Xiayu Xu, Kyungmoo Lee, Li Zhang, Milan Sonka, and Michael D Abràmoff. Stratified Sampling Voxel Classification for Segmentation of Intraretinal and Subretinal Fluid in Longitudinal Clinical OCT Data. *IEEE Transactions on Medical Imaging*, 34(7):1616–1623, 2015.

[40] Abhijit Guha Roy, Sailesh Conjeti, Sri Phani Krishna Karri, Debdoot Sheet, Amin Katouzian, Christian Wachinger, and Nassir Navab. ReLayNet: retinal layer and fluid segmentation of macular optical coherence tomography using fully convolutional networks. *Biomedical Optics Express*, 8(8):3627–3642, 2017.

[41] G N Girish, B Thakur, S R Chowdhury, A R Kothari, and J Rajan. Segmentation of Intra-Retinal Cysts From Optical Coherence Tomography Images Using a Fully Convolutional Neural Network Model. *IEEE Journal of Biomedical and Health Informatics*, 23(1):296–304, 2019.

[42] K Gopinath and J Sivaswamy. Segmentation of Retinal Cysts From Optical Coherence Tomography Volumes Via Selective Enhancement. *IEEE Journal of Biomedical and Health Informatics*, 23(1):273–282, 2019.

[43] G N Girish, Abhishek R. Kothari, and Jeny Rajan. Marker controlled watershed transform for intra-retinal cysts segmentation from optical coherence tomography B-scans. *Pattern Recognition Letters*, 139:86–94, 2020.

[44] Rhona Asgari, José Ignacio Orlando, Sebastian Waldstein, Ferdinand Schlanitz, Magdalena Baratsits, Ursula Schmidt-Erfurth, and Hrvoje Bogunović. Multiclass Segmentation as Multitask Learning for Drusen Segmentation in Retinal Optical Coherence Tomography BT - Medical Image Computing and Computer Assisted Intervention – MICCAI 2019. pages 192–200, Cham, 2019. Springer International Publishing.

[45] U Schmidt-Erfurth, S M Waldstein, S Klimscha, A Sadeghipour, X Hu, B S Gerendas, A Osborne, and H Bogunović. Prediction of individual disease conversion in early AMD using artificial intelligence. *Investigative Ophthalmology and Visual Science*, 59(8):3199–3208, 2018.

[46] Sina Farsiu, Stephanie J Chiu, Rachelle V O'Connell, Francisco A Folgar, Eric Yuan, Joseph A Izatt, Cynthia A Toth, Age-Related Eye Disease Study 2 Ancillary Spectral Domain Optical Coherence Tomography Study Group, and Others. Quantitative classification of eyes with and without intermediate age-related macular degeneration using optical coherence tomography. *Ophthalmology*, 121(1):162–172, 2014.

[47] Christian Simader, Jing Wu, Ana-Maria Glodan, Sebastian M Waldstein, Bianca S Gerendas, Georg Langs, Ursula Schmidt-Erfurth, and OPTIMA Segmentation Challenge. A Multi-vendor Dataset and Standardized Evaluation Framework for Retinal Cyst Segmentation. *Investigative Ophthalmology & Visual Science*, 56(7):5279, 2015.

[48] H Bogunović, F Venhuizen, S Klimscha, S Apostolopoulos, A Bab-Hadiashar, U Bagci, M F Beg, L Bekalo, Q Chen, C Ciller, K Gopinath, A K Gostar, K Jeon, Z Ji, S H Kang, D D Koozekanani, D Lu, D Morley, K K Parhi, H S Park, A Rashno, M Sarunic, S Shaikh, J Sivaswamy, R Tennakoon, S Yadav, S De Zanet, S M Waldstein, B S Gerendas, C Klaver, C I Sánchez, and U Schmidt-Erfurth. RETOUCH: The Retinal OCT Fluid Detection and Segmentation Benchmark and Challenge. *IEEE Transactions on Medical Imaging*, 38(8):1858–1874, 2019.

[49] Xiaoming Liu, Tianyu Fu, Zhifang Pan, Dong Liu, Wei Hu, and Bo Li. Semi-Supervised Automatic Layer and Fluid Region Segmentation of Retinal Optical Coherence Tomography Images Using Adversarial Learning. In *2018 25th IEEE International Conference on Image Processing (ICIP)*, pages 2780–2784, 2018.

[50] Donghuan Lu, Morgan Heisler, Sieun Lee, Gavin Weiguang Ding, Eduardo Navajas, Marinko V Sarunic, and Mirza Faisal Beg. Deep-learning based multiclass retinal fluid segmentation and detection in optical coherence tomography images using a fully convolutional neural network. *Medical Image Analysis*, 54:100–110, 2019.

[51] Daniel S Kermany, Michael Goldbaum, Wenjia Cai, Carolina C S Valentim, Huiying Liang, Sally L Baxter, Alex McKeown, Ge Yang, Xiaokang Wu, Fangbing Yan, and Others. Identifying medical diagnoses and treatable diseases by image-based deep learning. *Cell*, 172(5):1122–1131, 2018.

[52] Meng-Xiao Li, Su-Qin Yu, Wei Zhang, Hao Zhou, Xun Xu, Tian-Wei Qian, and Yong-Jing Wan. Segmentation of retinal fluid based on deep learning: application of three-dimensional fully convolutional neural networks in optical coherence tomography images. *International journal of ophthalmology*, 12(6):1012, 2019.

[53] Hao Wei and Peng Peng. The Segmentation of Retinal Layer and Fluid in SD-OCT Images Using Mutex Dice Loss Based Fully Convolutional Networks. *IEEE Access*, 8:60929–60939, 2020.

[54] Nihaal Mehta, Cecilia S Lee, Luísa S M Mendonça, Khadija Raza, Phillip X Braun, Jay S Duker, Nadia K Waheed, and Aaron Y Lee. Model-to-Data Approach for Deep Learning in Optical Coherence Tomography Intraretinal Fluid Segmentation. *JAMA Ophthalmology*, 138(10):1017–1024, oct 2020.

[55] Khaled Alsaih, Mohd Zuki Yusoff, Tong Boon Tang, Ibrahima Faye, and Fabrice Mériaudeau. Deep learning architectures analysis for age-related macular degeneration segmentation on optical coherence tomography scans. *Computer methods and programs in biomedicine*, 195:105566, 2020.

[56] K Alsaih, M Z Yusoff, T B Tang, I Faye, and F Mériaudeau. Retinal Fluids Segmentation Using Volumetric Deep Neural Networks on Optical Coherence Tomography Scans. In *2020 10th IEEE International Conference on Control System, Computing and Engineering (ICCSCE)*, pages 68–72, 2020.

[57] Sung Ho Kang, Hyoung Suk Park, Jaeseong Jang, and Kiwan Jeon. Deep neural networks for the detection and segmentation of the retinal fluid in OCT images. 2018.

[58] Kun Gao, Sijie Niu, Zexuan Ji, Menglin Wu, Qiang Chen, Rongbin Xu, Songtao Yuan, Wen Fan, Yuehui Chen, and Jiwen Dong. Double-branched and area-constraint fully convolutional networks for automated serous retinal detachment segmentation in SD-OCT images. *Computer Methods and Programs in Biomedicine*, 176:69–80, 2019.

[59] Liling Guan, Kai Yu, and Xinjian Chen. Fully automated detection and quantification of multiple retinal lesions in OCT volumes based on deep learning and improved DRLSE. In *Proc.SPIE*, volume 10949, mar 2019.

[60] Retinal Diseases and VISION 2020. *Community eye health*, 16(46):19–20, 2003.

[61] Oscar Julian Perdomo Charry and Fabio Augusto González Osorio. Una revisión sistemática de métodos de aprendizaje profundo aplicados a imágenes oculares. *Ciencia e Ingeniería Neogranadina*, 30(1 SE - Artículos):9–26, nov 2019.

[62] M Pekala, N Joshi, T Y Alvin Liu, N M Bressler, D Cabrera DeBuc, and P Burlina. Deep learning based retinal OCT segmentation. *Computers in Biology and Medicine*, 114:103445, 2019.

[63] Giacomo Panozzo and Andrea Mercanti. Optical Coherence Tomography Findings in Myopic Traction Maculopathy. *Archives of Ophthalmology*, 122(10):1455–1460, oct 2004.

[64] Oscar Perdomo, Hernán Rios, Francisco J Rodr´, Sebastián Otálora, Fabrice Meriaudeau, Henning Müller, and Fabio A González. Classification of diabetes-related retinal diseases using a deep learning approach in optical coherence tomography. *Computer methods and programs in biomedicine*, 178:181–189, 2019.

[65] Kevis-Kokitsi Maninis, Jordi Pont-Tuset, Pablo Arbeláez, and Luc Van Gool. Deep Retinal Image Understanding. *arXiv*, sep 2016.

[66] Joseph Redmon and Ali Farhadi. YOLOv3: An Incremental Improvement. *arXiv*, apr 2018.

[67] Phillip Isola, Jun-Yan Zhu, Tinghui Zhou, and Alexei A Efros. Image-to-Image Translation with Conditional Adversarial Networks, 2016.

[68] Stephanie J Chiu, Michael J Allingham, Priyatham S Mettu, Scott W Cousins, Joseph A Izatt, and Sina Farsiu. Kernel regression based segmentation of optical coherence tomography images with diabetic macular edema. *Biomedical optics express*, 6(4):1172–1194, mar 2015.

[69] Daniel Shu Wei Ting, Louis R Pasquale, Lily Peng, John Peter Campbell, Aaron Y Lee, Rajiv Raman, Gavin Siew Wei Tan, Leopold Schmetterer, Pearse A Keane, and Tien Yin Wong. Artificial intelligence and deep learning in ophthalmology. *British Journal of Ophthalmology*, 103(2):167–175, 2019.

[70] Alejandra Daruich, Alexandre Matet, Alexandre Moulin, Laura Kowalczuk, Michaël Nicolas, Alexandre Sellam, Pierre-Raphaël Rothschild, Samy Omri, Emmanuelle Gélizé, Laurent Jonet, Kimberley Delaunay, Yvonne De Kozak, Marianne Berdugo, Min Zhao, Patricia Crisanti, and Francine Behar-Cohen. Mechanisms of macular edema: Beyond the surface. *Progress in Retinal and Eye Research*, 63:20–68, 2018.

[71] Seth R Flaxman, Rupert R A Bourne, Serge Resnikoff, Peter Ackland, Tasanee Braithwaite, Maria V Cicinelli, Aditi Das, Jost B Jonas, Jill Keeffe, John H Kempen, Janet Leasher, Hans Limburg, Kovin Naidoo, Konrad Pesudovs, Alex Silvester, Gretchen A Stevens, Nina Tahhan, Tien Y Wong, Hugh R Taylor, Rupert Bourne, Peter Ackland, Aries Arditi, Yaniv Barkana, Banu Bozkurt, Tasanee Braithwaite, Alain Bron, Donald Budenz, Feng Cai, Robert Casson, Usha Chakravarthy, Jaewan Choi, Maria Vittoria Cicinelli, Nathan Congdon, Reza Dana, Rakhi Dandona, Lalit Dandona, Aditi Das, Iva Dekaris, Monte Del Monte, Jenny Deva, Laura Dreer, Leon Ellwein, Marcela Frazier, Kevin Frick, David Friedman, Joao Furtado, Hua Gao, Gus Gazzard, Ronnie George, Stephen Gichuhi, Victor Gonzalez, Billy Hammond, Mary Elizabeth Hartnett, Minguang He, James Hejtmancik, Flavio Hirai, John Huang, April Ingram, Jonathan Javitt, Jost Jonas, Charlotte Joslin, Jill Keeffe, John Kempen, Moncef Khairallah, Rohit Khanna, Judy Kim, George Lambrou, Van Charles Lansingh, Paolo Lanzetta, Janet Leasher, Jennifer Lim, Hans LIMBURG, Kaweh Mansouri, Anu Mathew, Alan Morse, Beatriz Munoz, David Musch, Kovin Naidoo, Vinay Nangia, Maria Palaiou, Maurizio Battaglia Parodi, Fernando Yaacov Pena, Konrad Pesudovs, Tunde Peto, Harry Quigley, Murugesan Raju, Pradeep Ramulu, Zane Rankin, Serge Resnikoff, Dana Reza,

Alan Robin, Luca Rossetti, Jinan Saaddine, Mya Sandar, Janet Serle, Tueng Shen, Rajesh Shetty, Pamela Sieving, Juan Carlos Silva, Alex Silvester, Rita S Sitorus, Dwight Stambolian, Gretchen Stevens, Hugh Taylor, Jaime Tejedor, James Tielsch, Miltiadis Tsilimbaris, Jan van Meurs, Rohit Varma, Gianni Virgili, Ya Xing Wang, Ning-Li Wang, Sheila West, Peter Wiedemann, Tien Wong, Richard Wormald, and Yingfeng Zheng. Global causes of blindness and distance vision impairment 1990x2013;2020: a systematic review and meta-analysis. *The Lancet Global Health*, 5(12):e1221–e1234, dec 2017.

[72] Undurti N Das. Diabetic macular edema, retinopathy and age-related macular degeneration as inflammatory conditions. *Archives of medical science : AMS*, 12(5):1142–1157, oct 2016.

[73] Mark W Johnson. Etiology and Treatment of Macular Edema. *American Journal of Ophthalmology*, 147(1):11–21.e1, 2009.

[74] Neelakshi Bhagat, Ruben A Grigorian, Arthur Tutela, and Marco A Zarbin. Diabetic Macular Edema: Pathogenesis and Treatment. *Survey of Ophthalmology*, 54(1):1–32, 2009.

[75] Matthias Bolz, Katharina Kriechbaum, Christian Simader, Gabor Deak, Jan Lammer, Clara Treu, Christoph Scholda, Christian Prünte, and Ursula Schmidt-Erfurth. In Vivo Retinal Morphology after Grid Laser Treatment in Diabetic Macular Edema. *Ophthalmology*, 117(3):538–544, 2010.

[76] Maurizio Battaglia Parodi and Francesco Bandello. Branch retinal vein occlusion: classification and treatment. *Ophthalmologica*, 223(5):298–305, 2009.

[77] Marion Funk, Katharina Kriechbaum, Franz Prager, Thomas Benesch, Michael Georgopoulos, Gerhard J Zlabinger, and Ursula Schmidt-Erfurth. Intraocular Concentrations of Growth Factors and Cytokines in Retinal Vein Occlusion and the Effect of Therapy with Bevacizumab. *Investigative Ophthalmology  Visual Science*, 50(3):1025–1032, mar 2009.

[78] Paris G Tranos, Sanjeewa S Wickremasinghe, Nikos T Stangos, Fotis Topouzis, Ioannis Tsinopoulos, and Carlos E Pavesio. Macular edema. *Survey of Ophthalmology*, 49(5):470–490, 2004.

[79] Marion R Munk, Stefan Sacu, Wolfgang Huf, Florian Sulzbacher, Tamara J Mittermüller, Katharina Eibenberger, Sandra Rezar, Matthias Bolz, Christopher G Kiss, Christian Simader, and Others. Differential diagnosis of macular edema of different pathophysiologic origins by spectral domain optical coherence tomography. *Retina*, 34(11):2218–2232, 2014.

[80] Robert T Atkinson Jr, Arthur J and Colburn, Wayne A and DeGruttola, Victor G and DeMets, David L and Downing, Gregory J and Hoth, Daniel F and Oates, John A and Peck, Carl C and Schooley. Biomarkers and surrogate endpoints: Preferred definitions and conceptual framework. *Clinical Pharmacology  Therapeutics*, 69(3):89–95, mar 2001.

[81] Robert M Califf. Biomarker definitions and their applications. *Experimental Biology and Medicine*, 243(3):213–221, 2018.

[82] Tso-Ting Lai, Yi-Ting Hsieh, Chung-May Yang, Tzyy-Chang Ho, and Chang-Hao Yang. Biomarkers of optical coherence tomography in evaluating the treatment outcomes of neovascular age-related macular degeneration: a real-world study. *Scientific Reports*, 9(1):529, 2019.

[83] Changyow C Kwan and Amani A Fawzi. Imaging and Biomarkers in Diabetic Macular Edema and Diabetic Retinopathy. *Current Diabetes Reports*, 19(10):95, 2019.

[84] Hyungwoo Lee, Hyoik Jang, Youn A Choi, Hyung Chan Kim, and Hyewon Chung. Association Between Soluble CD14 in the Aqueous Humor and Hyperreflective Foci on Optical Coherence Tomography in Patients With Diabetic Macular Edema. *Investigative Ophthalmology  Visual Science*, 59(2):715–721, feb 2018.

[85] Glenn Yiu, R Joel Welch, Yinwen Wang, Zhe Wang, Pin-Wen Wang, and Zdenka Haskova. Spectral-Domain OCT Predictors of Visual Outcomes after Ranibizumab Treatment for Macular Edema Resulting from Retinal Vein Occlusion. *Ophthalmology Retina*, 4(1):67–76, 2020.

[86] D Jha, P H Smedsrud, M A Riegler, D Johansen, T D Lange, P Halvorsen, and H D. Johansen. ResUNet++: An Advanced Architecture for Medical Image Segmentation. In *2019 IEEE International Symposium on Multimedia (ISM)*, pages 225–230, 2019.

[87] Jie Hu, Li Shen, and Gang Sun. Squeeze-and-excitation networks. In *Proceedings of the IEEE conference on computer vision and pattern recognition*, pages 7132–7141, 2018.